MONASH University

3D meta-optics: a platform for wavefront shaping and optical sensing

Haoran Ren

ARC DECRA Fellow

School of Physics and Astronomy

Monash University

Email: haoran.ren@monash.edu

Web: https://rengroupnano.com/

REN GROUP

Light manipulation via ultrathin metasurfaces

N. Yu, et. al., Science. **334**, 333 (2011). S. Sun, et. al., Nano Lett. **12**, 6223 (2012).

Human hair

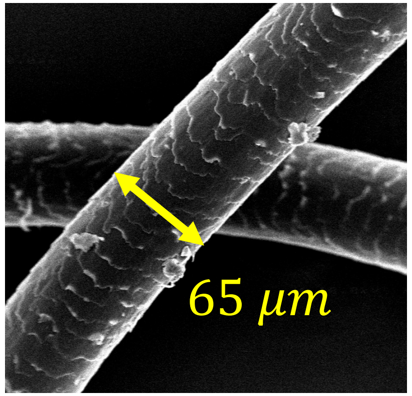

Metasurface

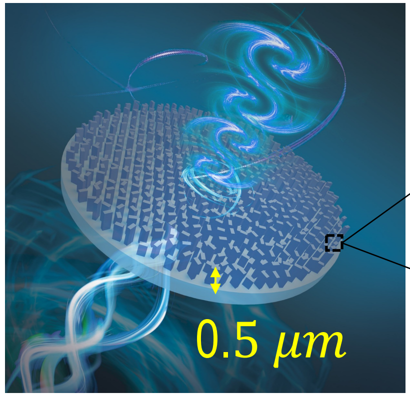

Meta-atom

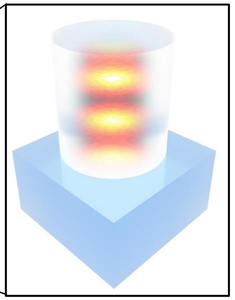

Arbitrary light steering

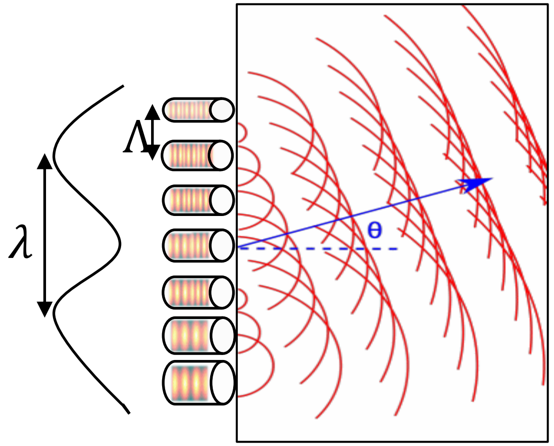

3D laser nanoprinted metasurfaces

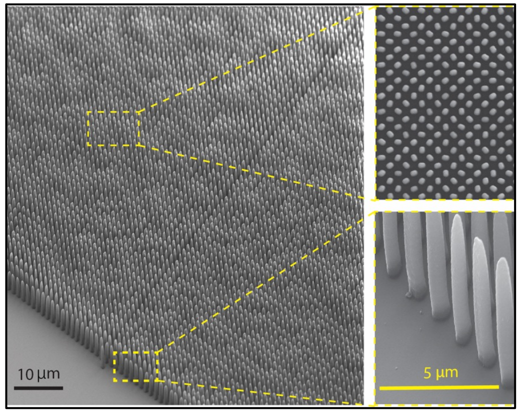

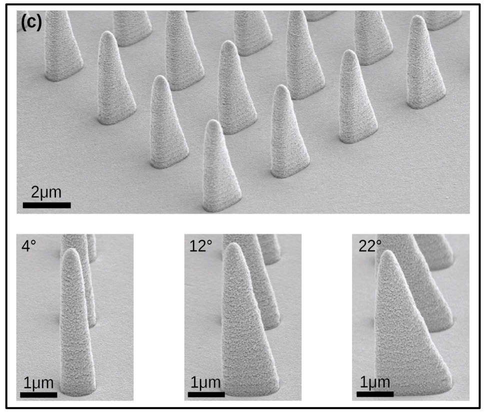

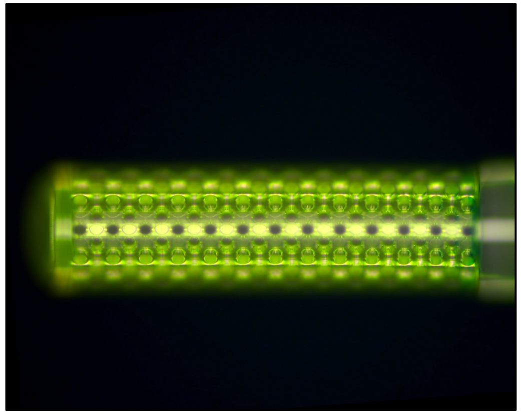

nanoscribe.com

MONASH University

MONASH University

Metasurface examples

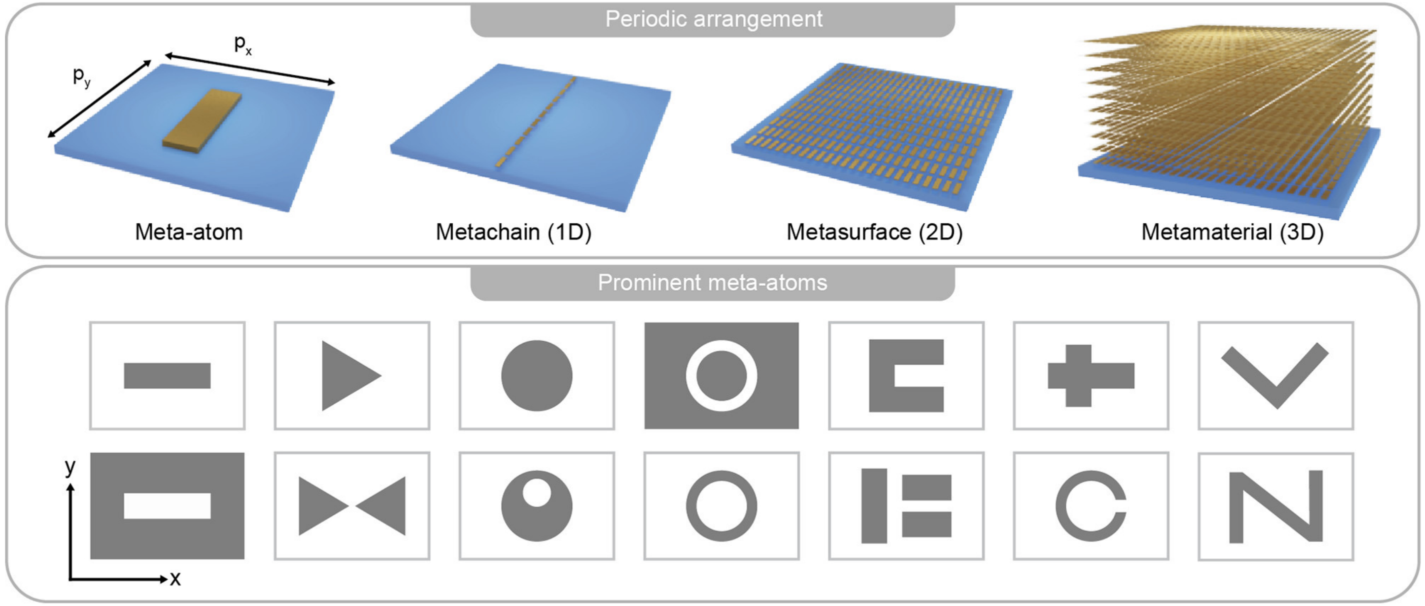

E. Cortes, F. J. Wendisch, L. Sortino, A. Mancini, S. Ezendam, S. Saris, L. D. S. Menezes, A. Tittl, H. Ren, S. A. Maier, Metasurfaces for energy conversion, *Chem. Rev.* 122, 15082–15176 (2022).

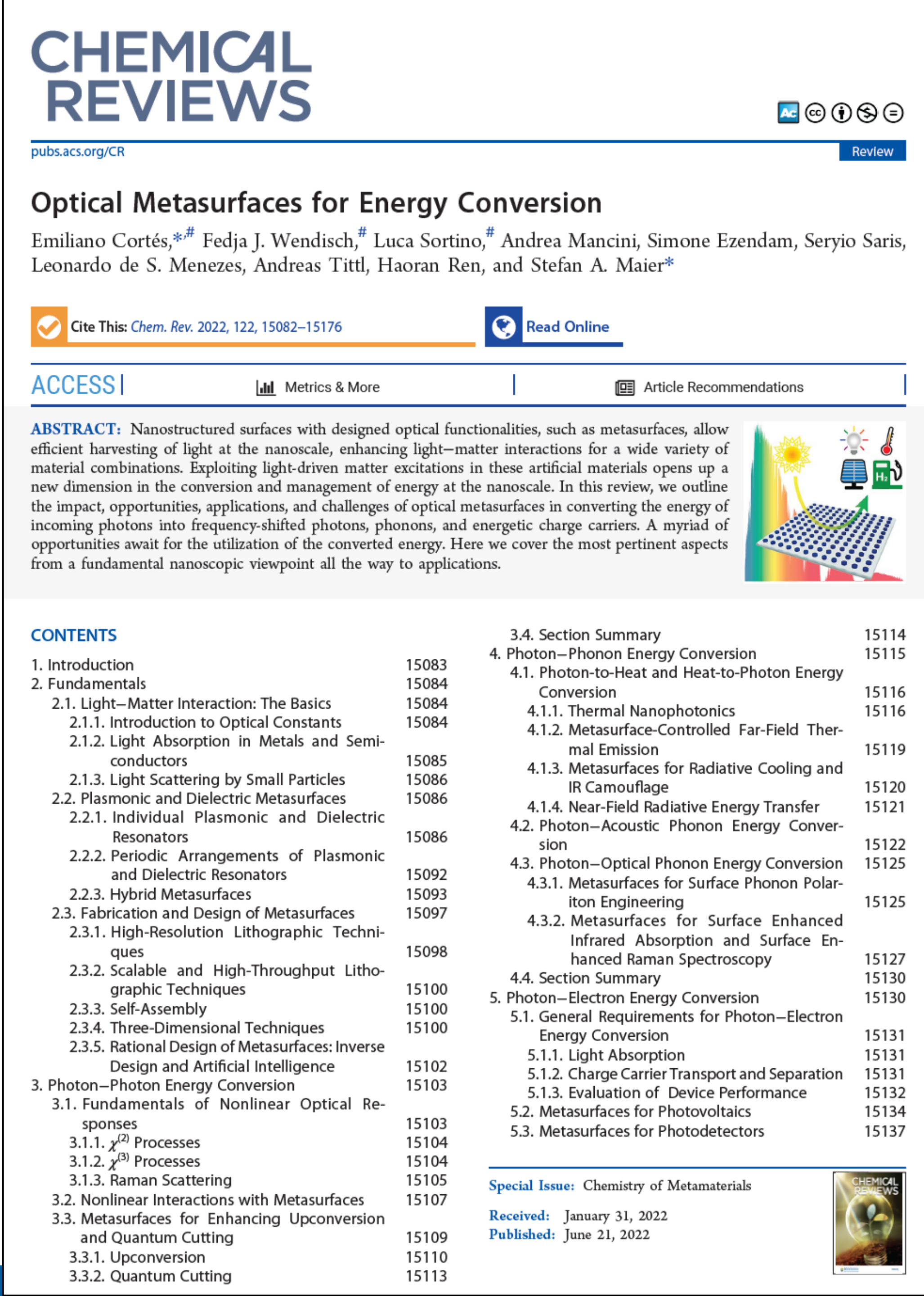

CHEMICAL REVIEWS
pubs.acs.org/CR
Review

Optical Metasurfaces for Energy Conversion

Emiliano Cortés,*,# Fedja J. Wendisch,# Luca Sortino,# Andrea Mancini, Simone Ezendam, Seryio Saris, Leonardo de S. Menezes, Andreas Tittl, Haoran Ren, and Stefan A. Maier*

Cite This: *Chem. Rev.* 2022, 122, 15082–15176

Read Online

ACCESS | Metrics & More | Article Recommendations

ABSTRACT: Nanostructured surfaces with designed optical functionalities, such as metasurfaces, allow efficient harvesting of light at the nanoscale, enhancing light–matter interactions for a wide variety of material combinations. Exploiting light-driven matter excitations in these artificial materials opens up a new dimension in the conversion and management of energy at the nanoscale. In this review, we outline the impact, opportunities, applications, and challenges of optical metasurfaces in converting the energy of incoming photons into frequency-shifted photons, phonons, and energetic charge carriers. A myriad of opportunities await for the utilization of the converted energy. Here we cover the most pertinent aspects from a fundamental nanoscopic viewpoint all the way to applications.

CONTENTS

Special Issue: Chemistry of Metamaterials
Received: January 31, 2022
Published: June 21, 2022

a. Far-field electromagnetic wave manipulation

➢ Resonance-based gradient metasurfaces

(a-b) Plasmonic resonance

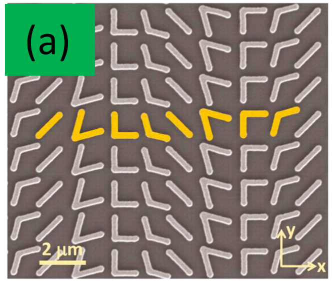

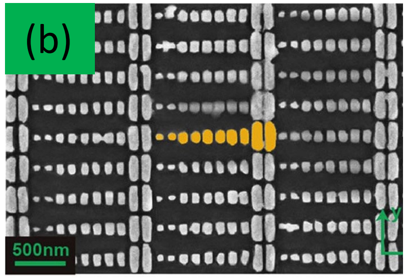

N. Yu, et. al., *Science* **334**, 333 (2011).
S. Sun, et. al., *Nat. Mater.* **11**, 426 (2012).
S. Sun, et. al., *Nano Lett.* **12**, 6223 (2012).

(c) Dielectric resonance

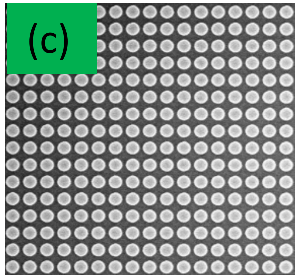

M. Decker, et. al., *Adv. Opt. Mater.* **3**, 813 (2015).

➢ High-quality-factor metasurfaces

(d) Fano-type interference

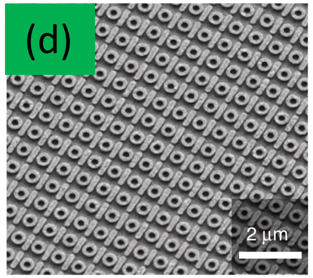

Y. Yang, et. al., *Nat. Commun.* **5**, 5753 (2014).

(e-f) Surface lattice resonance

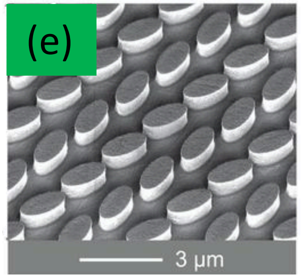

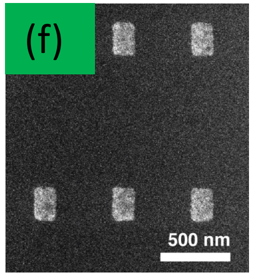

A. Tittl, et. al., *Science* **360**, 1105 (2018).
M. S. Bin-Alam, et. al., *Nat. Commun.* **12**, 974 (2021).

➢ Broadband geometric and hybrid metasurfaces

(g-h) Geometric metasurfaces

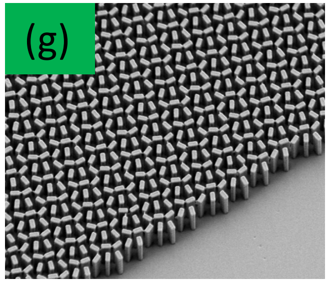

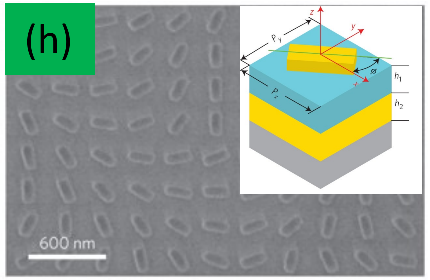

Z. Bomzon, et al., *Opt. Lett.* **27**, 1141 (2002). D. Lin, et. al., *Science* **345**, 298 (2014).
G. Zheng, et. al., *Nat. Nanotechnol.* **10**, 308 (2015).
M. Khorasaninejad, et. al., *Science* **352**, 1190 (2016).

(i-j) Hybrid metasurfaces

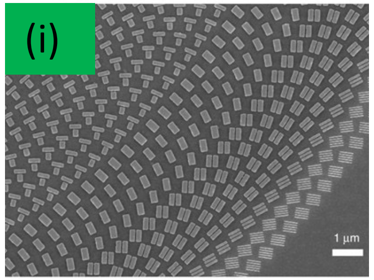

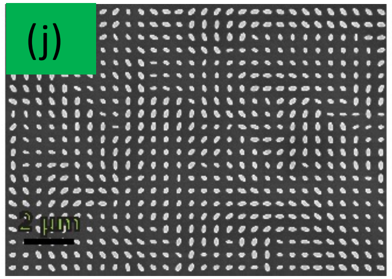

S. Wang, et. al., *Nat. Nanotechnol.* **13**, 227 (2018).
A. Arbabi, et. al., *Nat. Nanotechnol.* **10**, 937 (2015).
J. P. B. Mueller, et. al., *Phys. Rev. Lett.* **118**, 113901 (2017).

(k) 3D metasurfaces

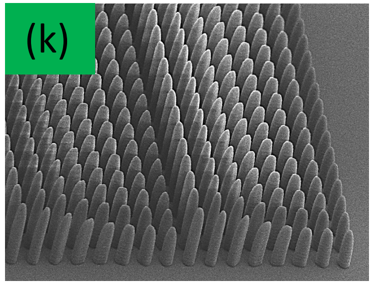

H. Ren, et. al., *Nat. Nanotechnol.* **15**, 948 (2020).

b. Near-field electromagnetic wave manipulation

(l-n) Wavelength-selective metasurfaces

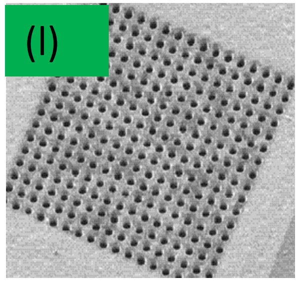

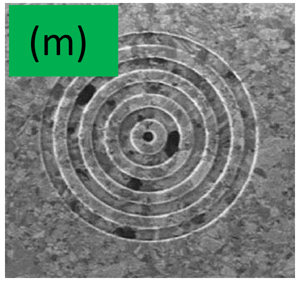

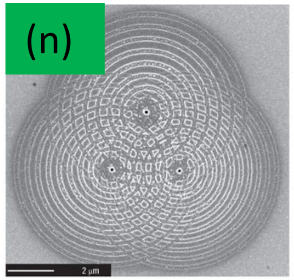

T. W. Ebbessen, et al., *Nature* **391**, 667 (1998).
H. J. Lezec, et al., *Science* **297**, 820 (2002).

E. Laux, et al., *Nat. Nanotechnol.* **2**, 161 (2008).
J. Lin, et al., *Science* **340**, 331 (2013).

(o-p) Polarization-selective metasurfaces

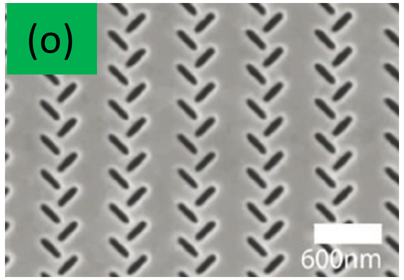

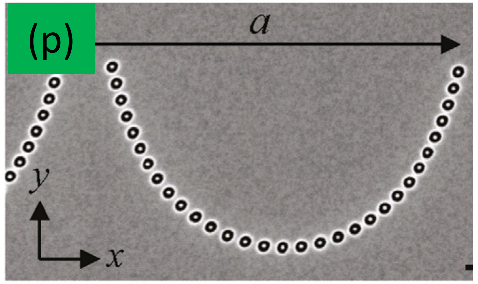

N. Shitrit, et al., *Nano Lett.* **11**, 2038 (2011).

(q) Orbital angular momentum-selective metasurfaces

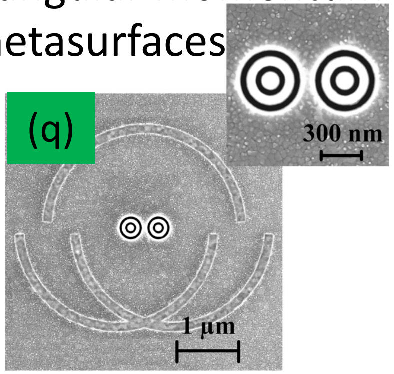

H. Ren, et al., *Science* **352**, 805 (2016).

3D laser printing – the beginning

OPTICS LETTERS / Vol. 22, No. 2 / January 15, 1997

Three-dimensional microfabrication with two-photon-absorbed photopolymerization

Shoji Maruo, Osamu Nakamura, and Satoshi Kawata

Department of Applied Physics, Osaka University, Suita, Osaka 565, Japan

Received October 1, 1996

We propose a method for three-dimensional microfabrication with photopolymerization stimulated by two-photon absorption with a pulsed infrared laser. An experimental system for the microfabrication has been developed with a Ti:sapphire laser whose oscillating wavelength and pulse width are 790 nm and 200 fs, respectively. The usefulness of the proposed method has been verified by fabrication of several kinds of microstructure by use of a resin consisting of photoinitiators, urethane acrylate monomers, and urethane acrylate oligomers.

brief communications

Finer features for functional microdevices

Micromachines can be created with higher resolution using two-photon absorption.

Compared with light or electron-beam lithography, the virtue of two-photon photopolymerization[1] as a tool for making microdevices lies in its three-dimensional capability, which has found application in photonic devices[2–4] and micromachines[1,5,6] with feature sizes close to the diffraction limit. Here we show that the diffraction limit can be exceeded by non-linear effects to give a subdiffraction-limit spatial resolution of 120 nanometres. This allows functional micromachines to be created and shifts the working wavelength of photonic and opto-electronic devices into the visible and near-infrared region.

Commercially available resin (SCR500; JSR, Japan), consisting of urethane acrylate monomers and oligomers as well as photo-initiators, is transparent to an infrared laser and allows it to penetrate deeply. The resin can be photopolymerized by using two-photon absorption (TPA)[7–9] to create three-dimensional structures. By pinpoint-scanning the laser focus according to pre-programmed patterns, designs can be faithfully replicated to matter structures.

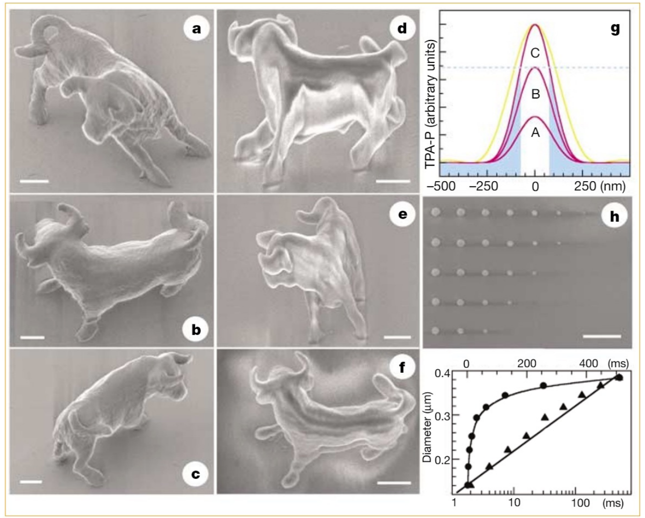

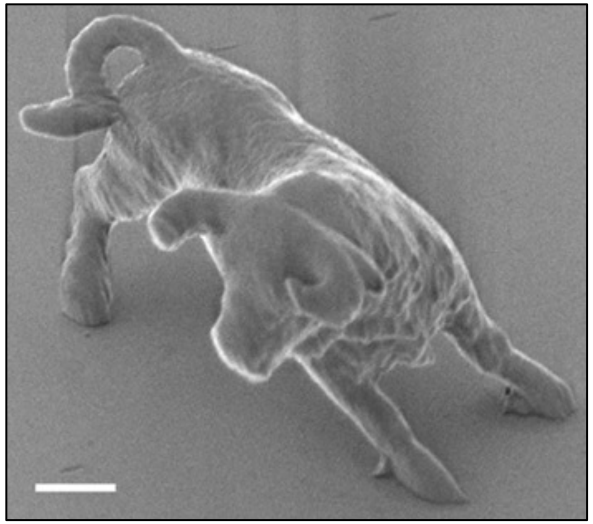

10 micrometers long bull

Nature **412**, 697–698 (2001)

Two-photon polymerisation

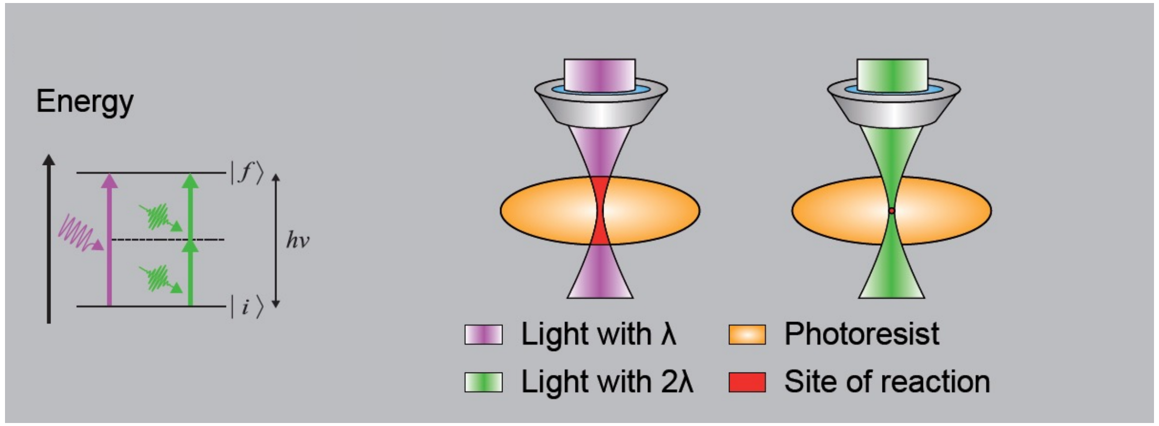

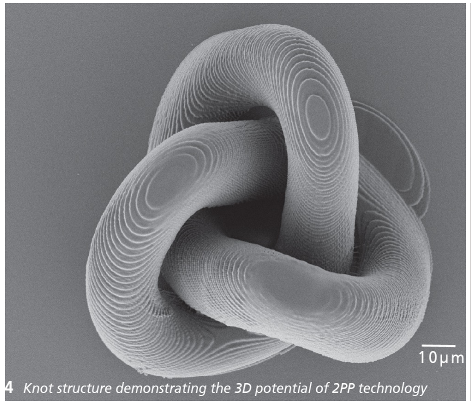

4 Knot structure demonstrating the 3D potential of 2PP technology

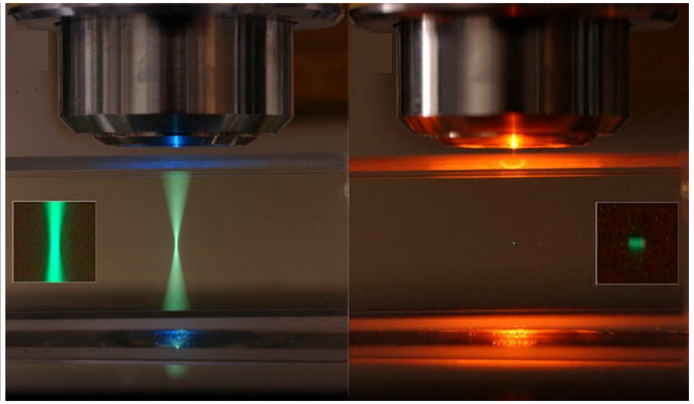

https://www.cesma.de/en/processing/two-photon-polymerization.html

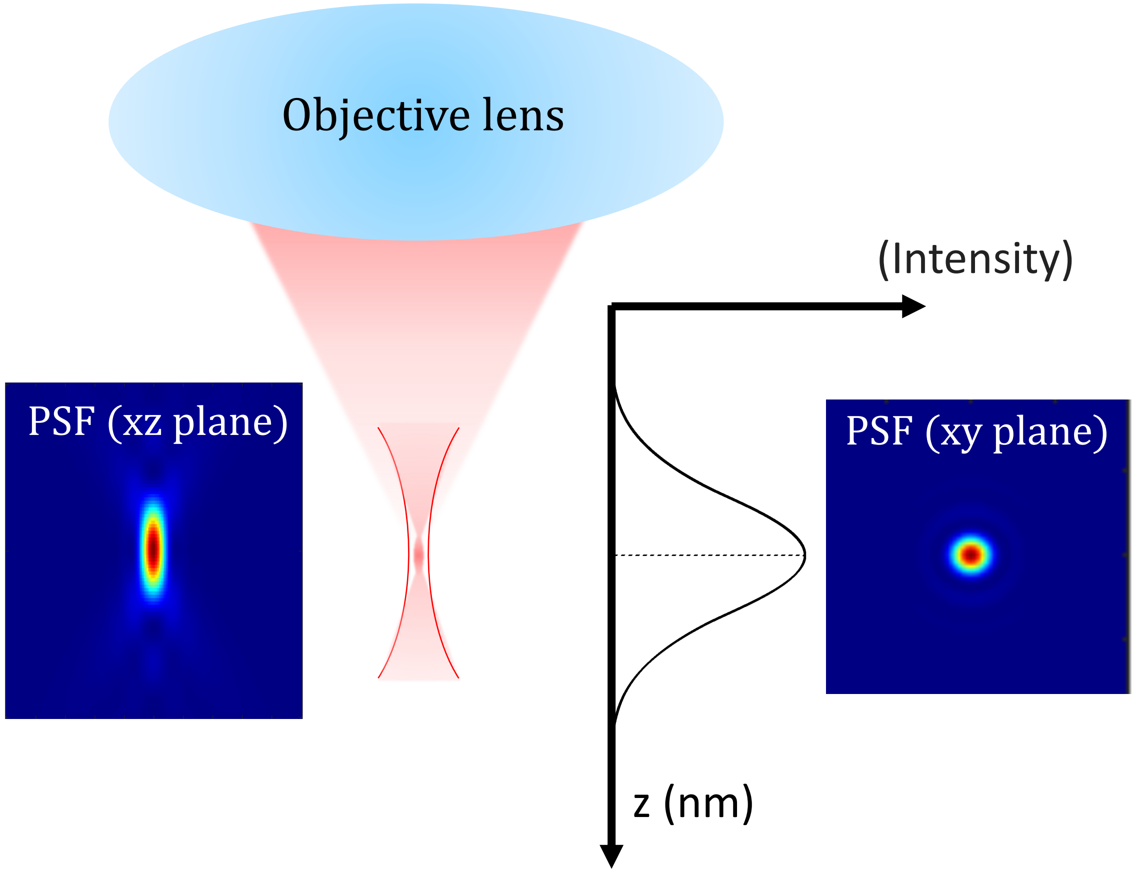

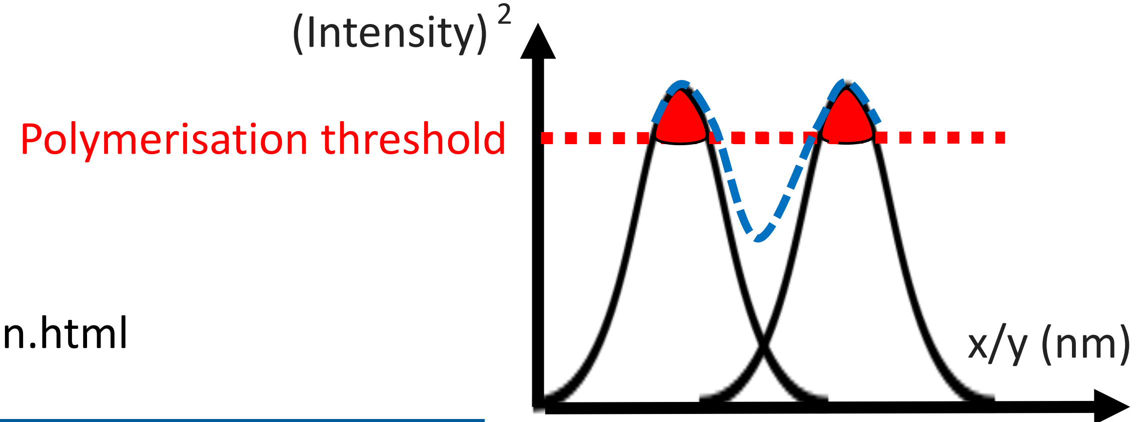

MONASH University

Metasurface design – dielectric modes

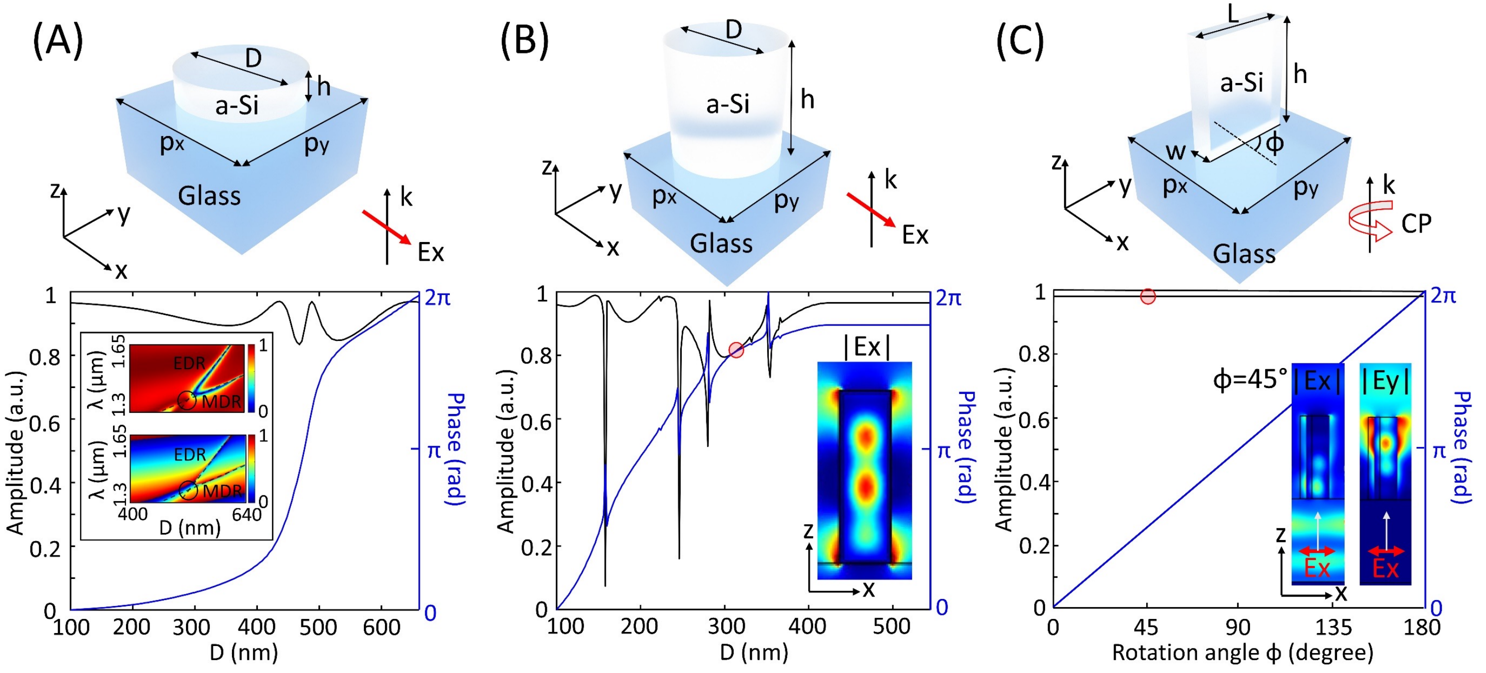

H. Ren, S. A. Maier, Nanophotonic materials for twisted-light manipulation, ***Adv. Mater.*** 2106692, (2022).

REVIEW

ADVANCED MATERIALS
www.advmat.de

Nanophotonic Materials for Twisted-Light Manipulation

Haoran Ren and Stefan A. Maier**

Twisted light, an unbounded set of helical spatial modes carrying orbital angular momentum (OAM), offers not only fundamental new insights into structured light–matter interactions, but also a new degree of freedom to boost optical and quantum information capacity. However, current OAM experiments still rely on bulky, expensive, and slow-response diffractive or refractive optical elements, hindering today's OAM systems to be largely deployed. In the last decade, nanophotonics has transformed the photonic design and unveiled a diverse range of compact and multifunctional nanophotonic devices harnessing the generation and detection of OAM modes. Recent metasurface devices developed for OAM generation in both real and momentum space, presenting design principle and exemplary devices, are summarized. Moreover, recent development of whispering-gallery-mode-based passive and tunable microcavities, capable of extracting degenerate OAM modes for on-chip vortex emission and lasing, is summarized. In addition, the design principle of different plasmonic devices and photodetectors recently developed for on-chip OAM detection is discussed. Current challenges faced by the nanophotonic field for twisted-light manipulation and future advances to meet these challenges are further discussed. It is believed that twisted-light manipulation in nanophotonics will continue to make significant impact on future development of ultracompact, ultrahigh-capacity, and ultrahigh-speed OAM systems-on-a-chip.

1. Introduction

The development of miniaturized photonic devices to generate, transmit, manipulate, and retrieve increasingly enormous amounts of data for high-capacity optical networks is vitally important. During the 1980s, optical communication experiments driven by wavelength-division multiplexing were performed on large optical tables using expensive devices that were not meant for practical communication systems. The development of cost-effective, integrated devices then followed, to enable wavelength-division multiplexing to be widely deployed. However, present-day optical communication systems using wavelength-division multiplexing are heading toward a capacity limit (**Figure 1**A). To further scale-up the capacity of photonic devices, twisted light multiplexing, based on an unbounded set of orbital angular momentum (OAM) modes, has been recognized as a viable space-division multiplexing approach to significantly increasing the multiplexing capacity of future optical communication systems.[1] In this context, OAM multiplexing has been employed for optical communications in free space,[2,3] optical fibers,[4] and quantum communications.[5–7] It should be mentioned, however, OAM modes are only a subset of the Laguerre–Gaussian modes of structured light,[8] and increasing optical multiplexing capacity can also be realized from other sets of orthogonal spatial modes.[9] However, owing to the fast growing OAM research field, a broad range of photonic devices used for the OAM generation, multiplexing, detection, and demultiplexing have been developed, offering the OAM a compelling advantage to be largely deployed in future photonic information systems.

The angular momentum is a property to describe the rotation of an object around an axis. When it applies to light beams, the angular momentum **L** can be defined as the cross-product between the position vector **r** and the linear momentum vector

$$\mathbf{L} = \varepsilon_0 \int \mathbf{r} \times (\mathbf{E} \times \mathbf{B}) d^3r \quad (1)$$

where ε_0 is the vacuum permittivity, **E** and **B** are the vectorial electric and magnetic fields of an electromagnetic wave. The angular momentum can be separated in the paraxial limit into two parts: the spin angular momentum (SAM) associated with circular polarization, and the OAM manifested by an optical vortex beam with a helical wavefront.[10] For both paraxial and

H. Ren
MQ Photonics Research Centre
Department of Physics and Astronomy
Macquarie University
Macquarie Park, NSW 2109, Australia
E-mail: haoran.ren@mq.edu.au
S. A. Maier
Chair in Hybrid Nanosystems
Nanoinstitute Munich
Faculty of Physics
Ludwig-Maximilians-University Munich
80539 Munich, Germany
E-mail: stefan.maier@physik.uni-muenchen.de
S. A. Maier
Department of Physics
Imperial College London
London SW7 2AZ, UK
The ORCID identification number(s) for the author(s) of this article can be found under https://doi.org/10.1002/adma.202106692.

DOI: 10.1002/adma.202106692

MONASH University

•Outline

- Complex-amplitude metasurface for twisted light holography

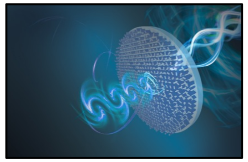

- Plasmonic nanofin metasurface for tailored molecular sensing

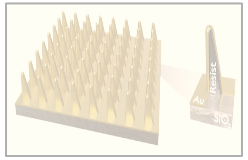

- Achromatic metafibre for broadband focusing and imaging

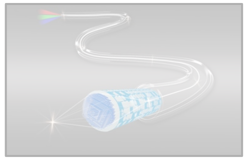

Optical and digital holography

https://www.pinterest.com/pin/289285976050552182/

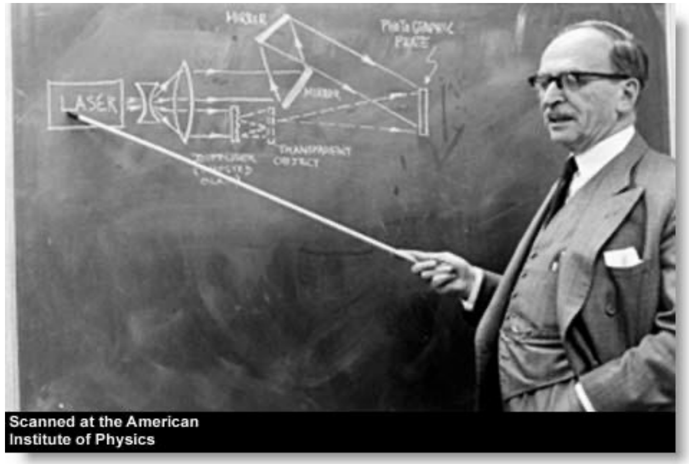

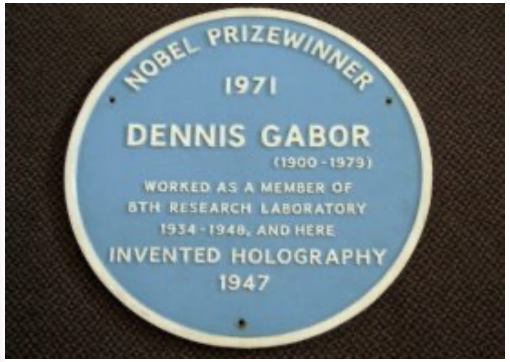

Optical holography

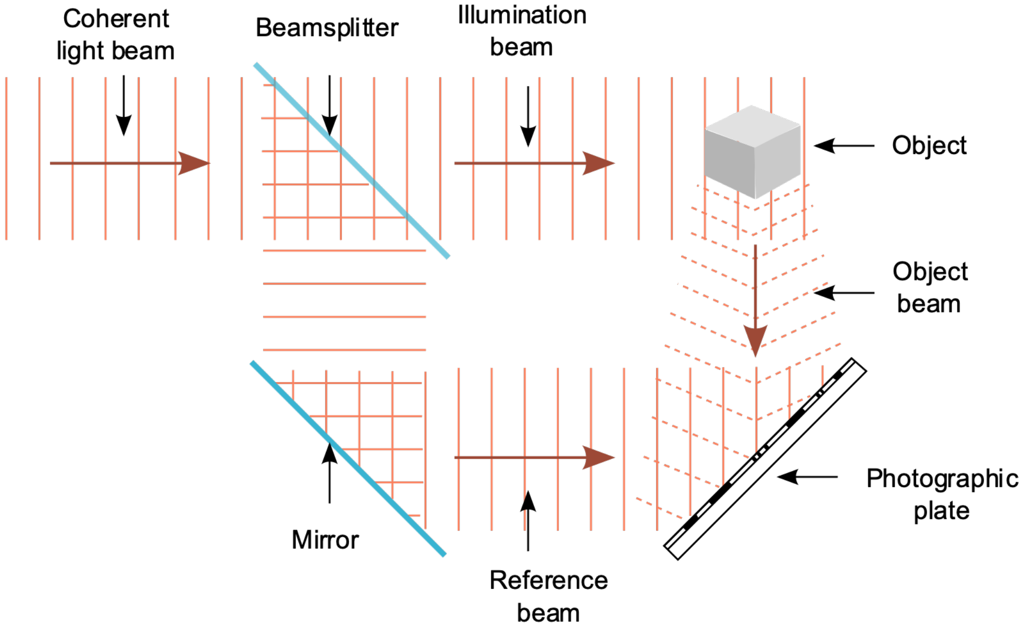

Released under public domain by http://en.wikipedia.org/wiki/User:Wykis

Digital holography

Computer

Computer-generated hologram

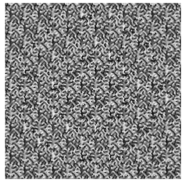

Direct display

Fabrication/printing

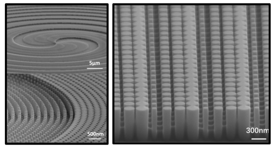

Multi-dimensional metasurface holography

Polarization multiplexing meta-hologram

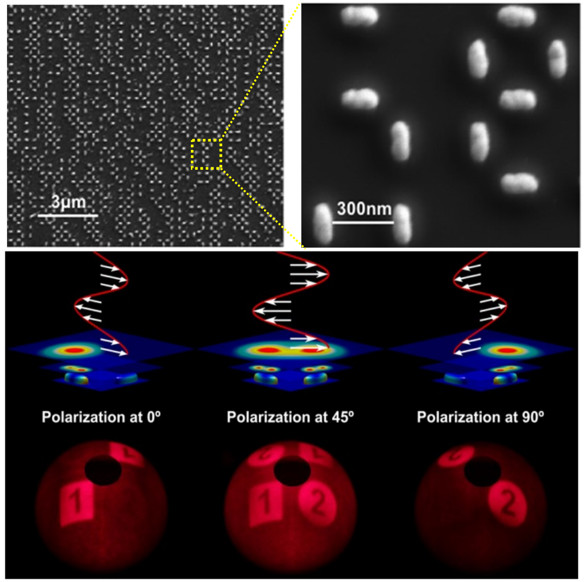

Nano. Lett. **14**, 294 (2013).

Spin angular momentum multiplexing meta-hologram

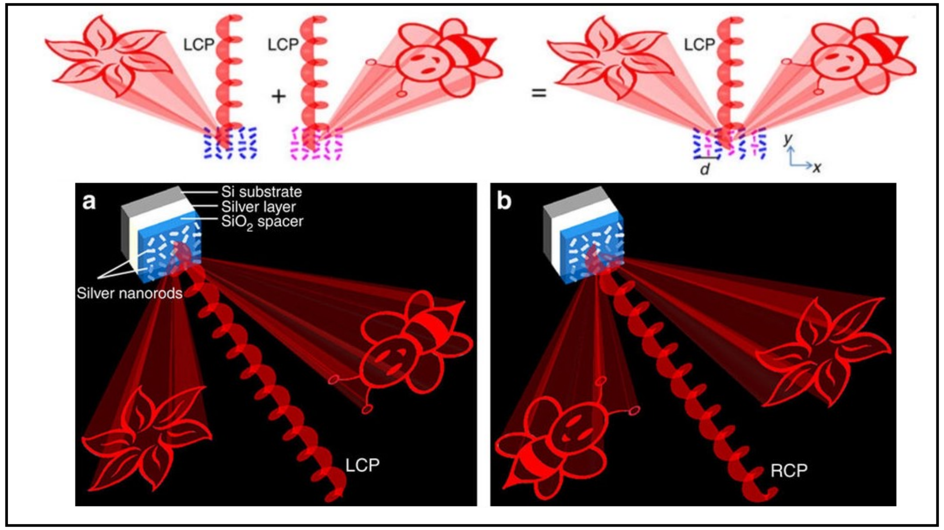

Nat. Commun. **6**, 8241 (2015).

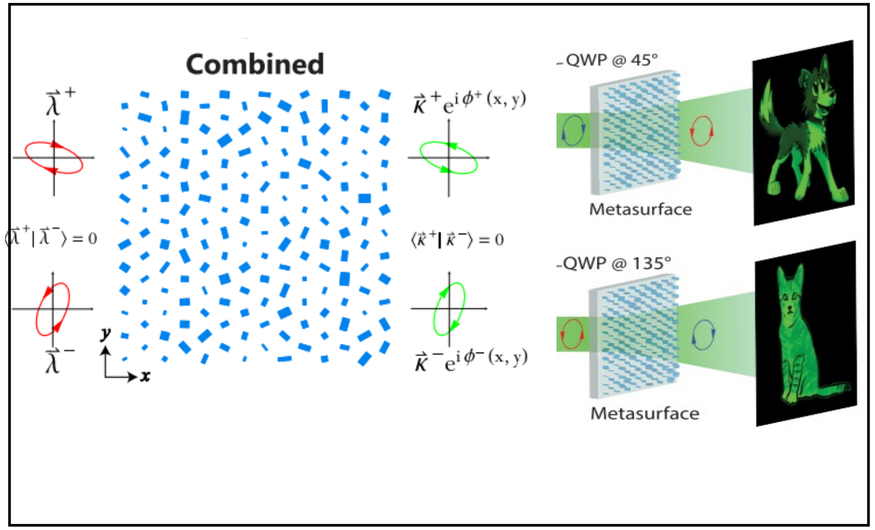

PRL **118**, 113901 (2017).

Wavelength multiplexing meta-hologram

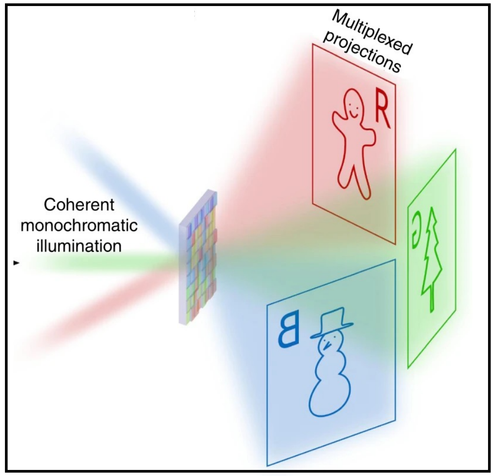

Nat. Commun. **7**, 11930 (2016).

Angle multiplexing meta-hologram

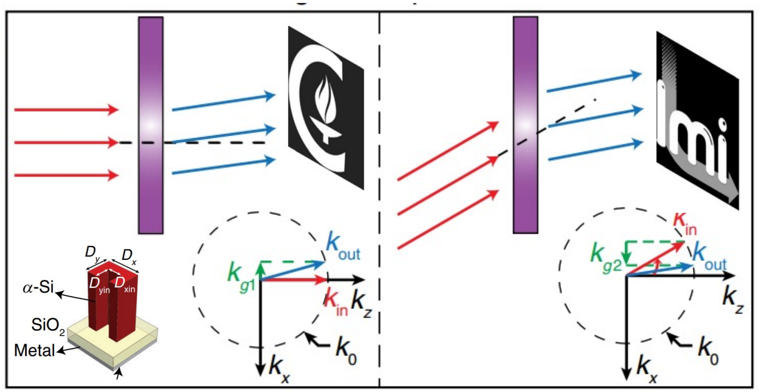

Phys. Rev. X. **7**, 041056 (2017).

Space channel meta-hologram

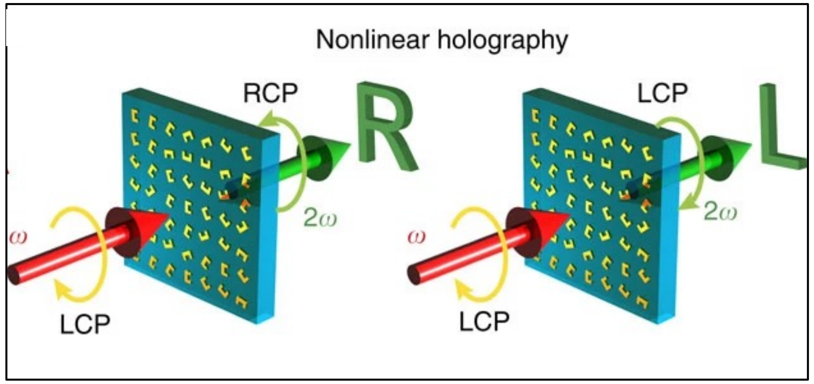

Nat. Commun. **7**, 11930 (2016).

Multi-dimensional light control

A light beam being spatially/temporarily structured in different degrees of freedom of light.

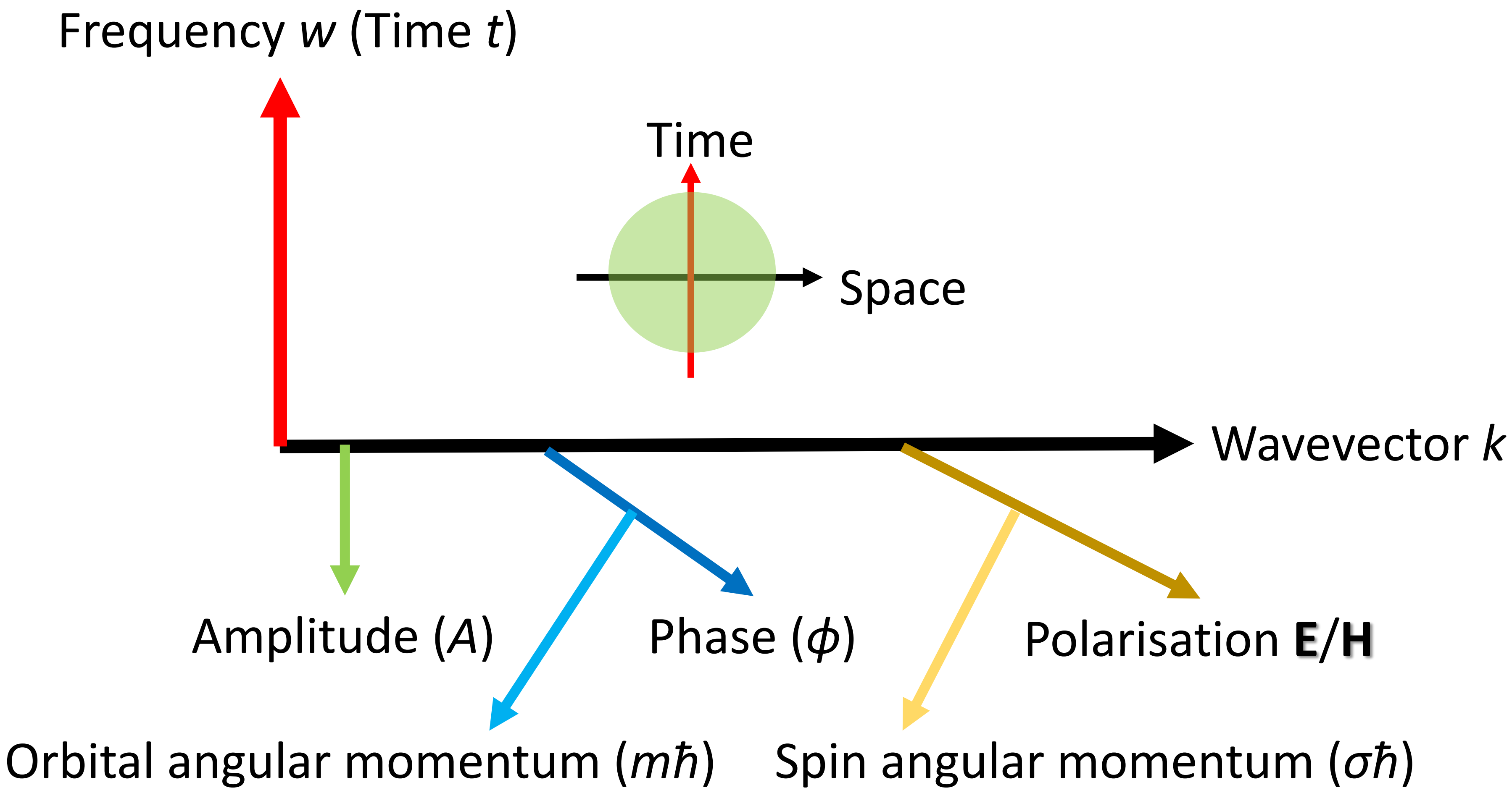

Why do we need structured light?

A light beam can be structured into millions of spatial modes in square millimetre

Structured light generation relies on bulky, heavy and expensive optical table systems

Vector beams   Twisted beams

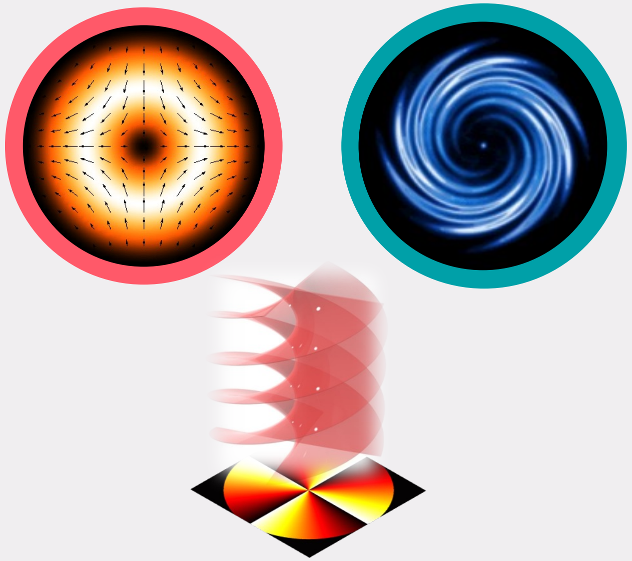

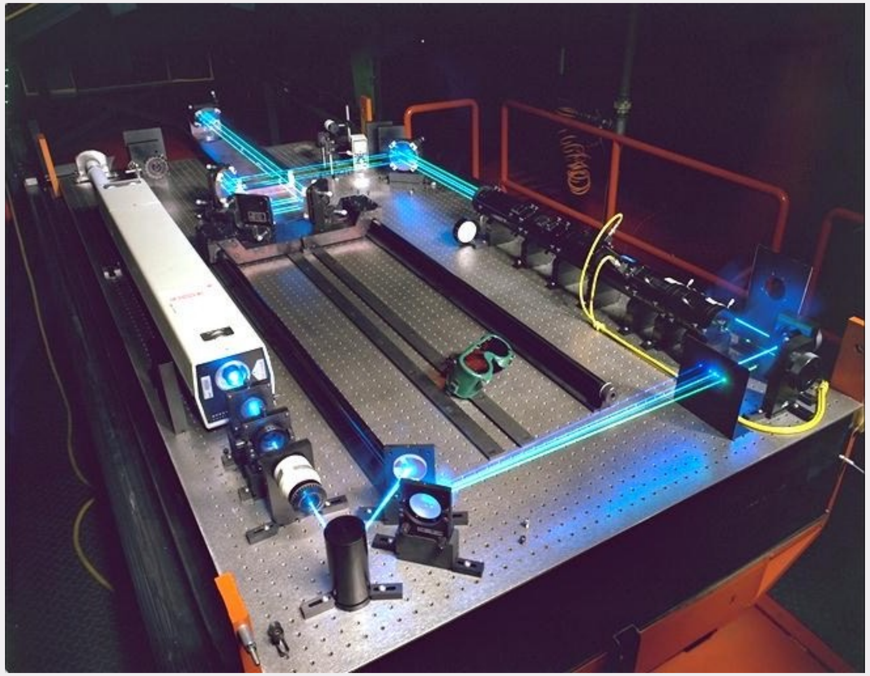

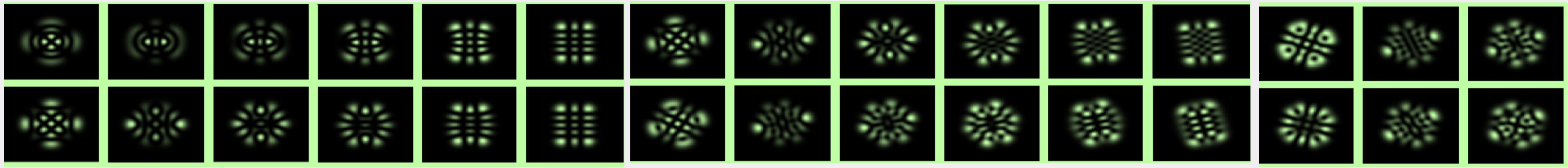

Angular momentum of light

Angular momentum: $\mathbf{j} = \mathbf{r} \times \mathbf{p}$

Linear momentum: $\mathbf{p} = \varepsilon_0 \mathbf{E} \times \mathbf{B}$

SAM: $s\hbar(s = -1, +1)$

OAM: $\ell\hbar(\ell : \pm 1, \pm 2, \pm 3 \ldots)$

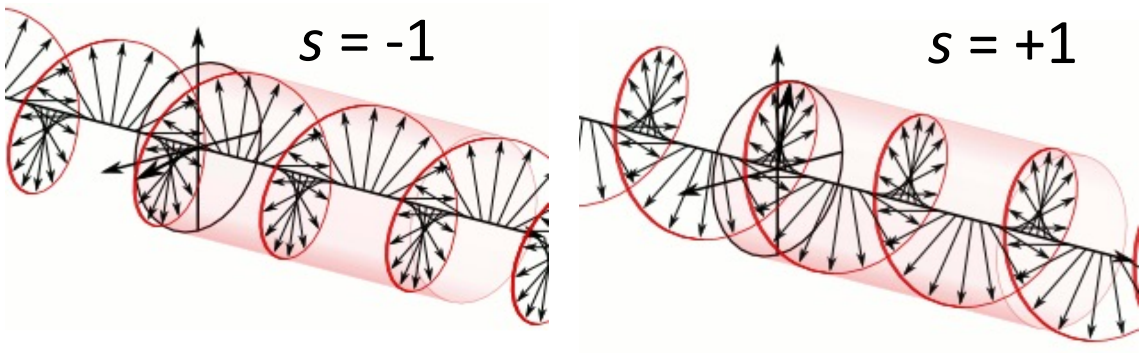

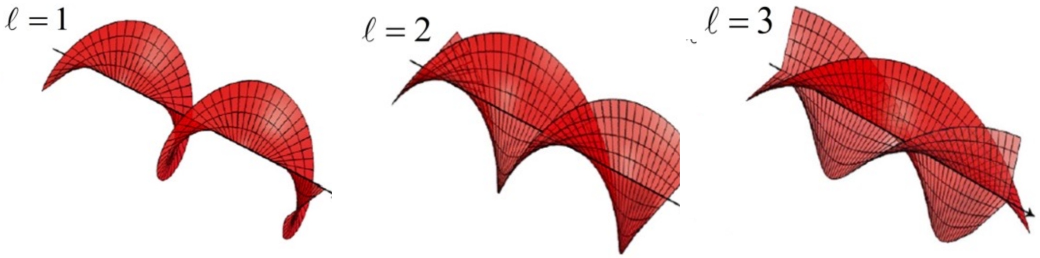

key features of orbital angular momentum (OAM):

✓**Unbounded OAM modes**

✓**Intrinsic modal orthogonality**

$U_1 = A_1(r, z)\exp(il_1\varphi) \quad U_2 = A_2(r, z)\exp(il_2\varphi)$

$$\int_0^{2\pi} U_1 U_2^* d\varphi = \begin{cases} 0 & if\ l_1 \neq l_2 \\ A_1 A_2^* & if\ l_1 = l_2 \end{cases}$$

L. Allen *et. al., Phys. Rev. A*, **45**, 11 (1992).

A. M. Yao et. al., *Adv. Opt. Photonics* **3**, 161-204 (2011).

OAM holography in the momentum space

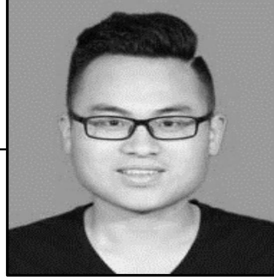

Conventional hologram

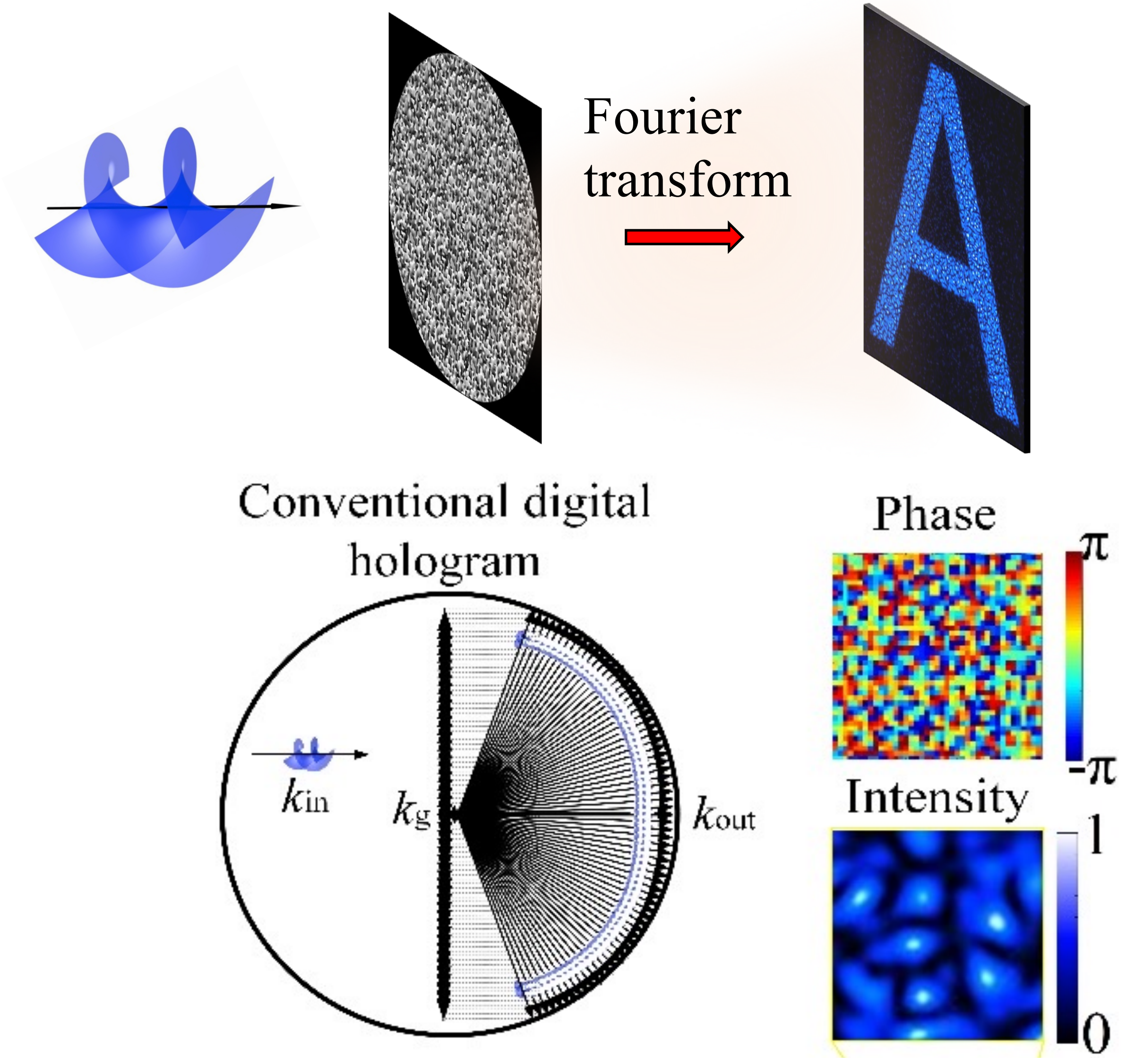

OAM-preserving hologram

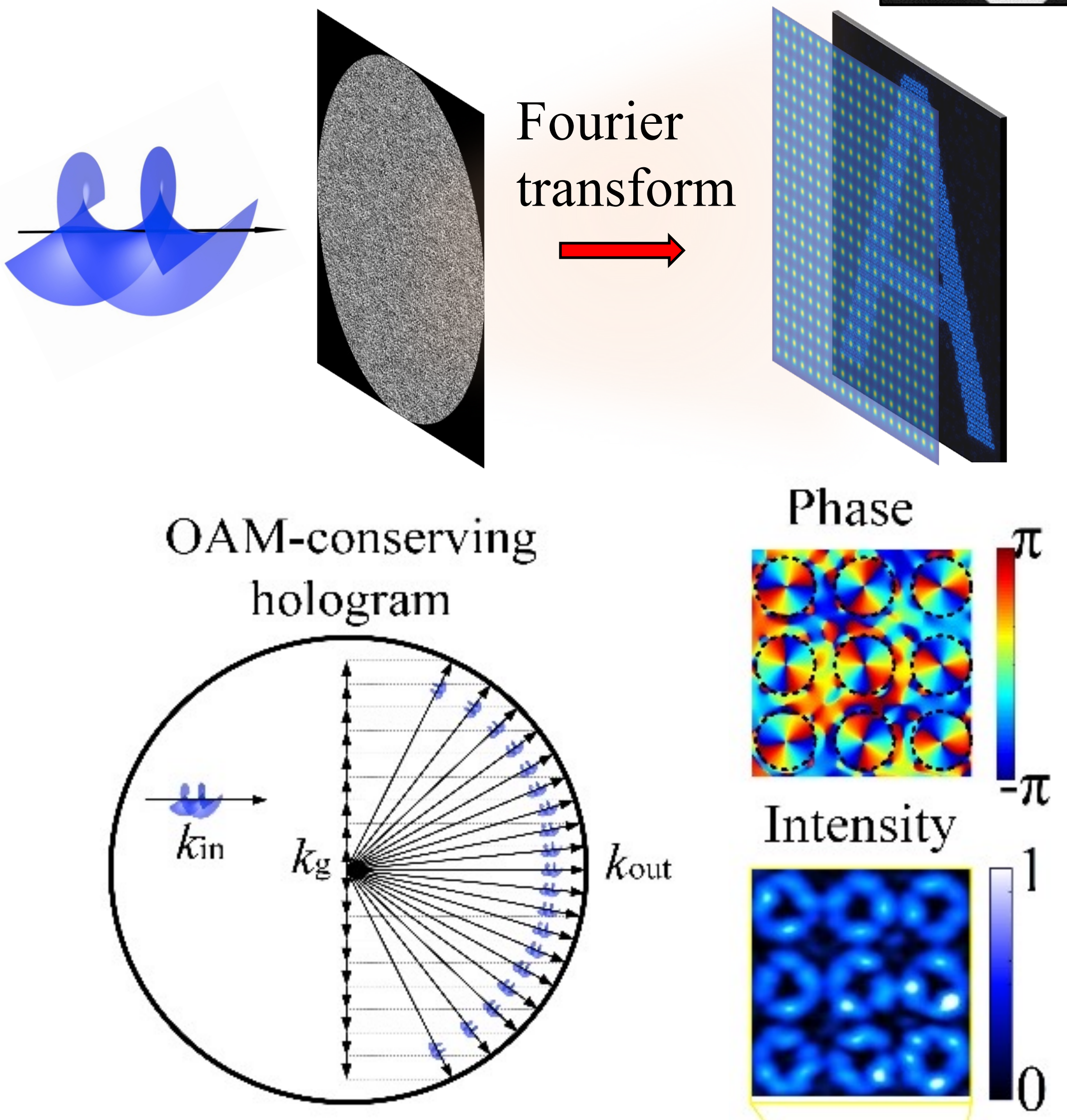

OAM holography in the momentum space

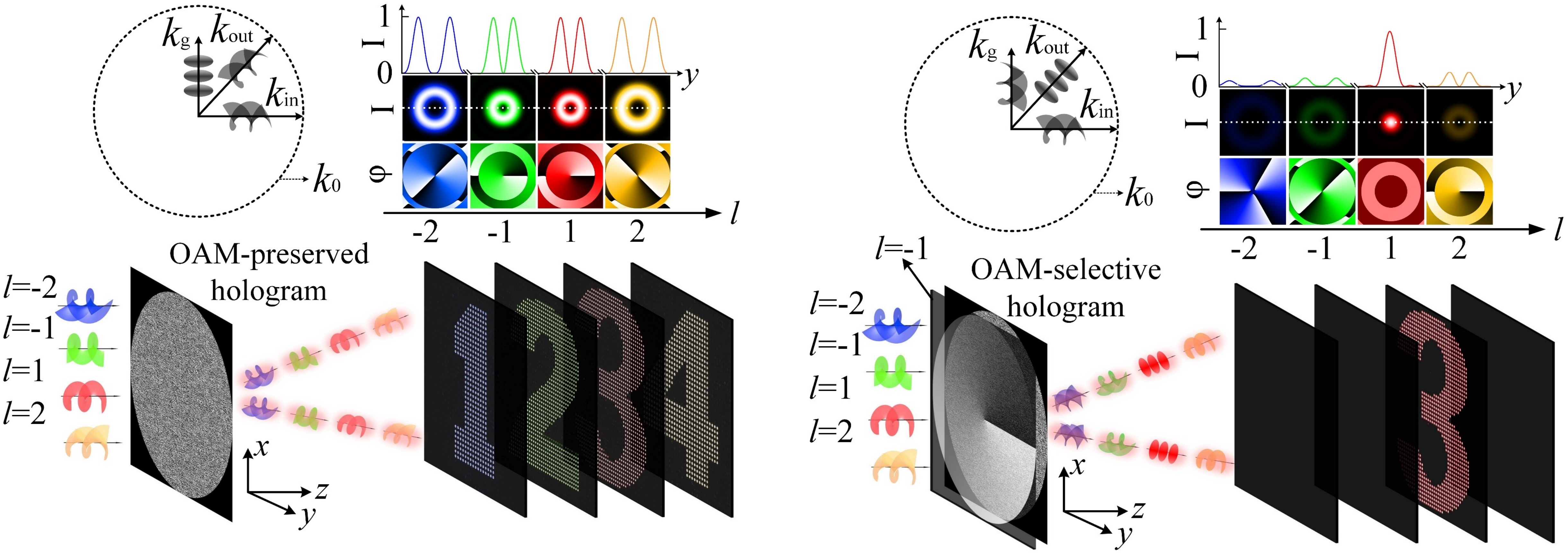

X. Fang, H. Ren, and M. Gu, Orbital angular momentum holography for high security encryption, *Nat. Photonics* **14**, 102-108 (2020).

OAM holography in the momentum space

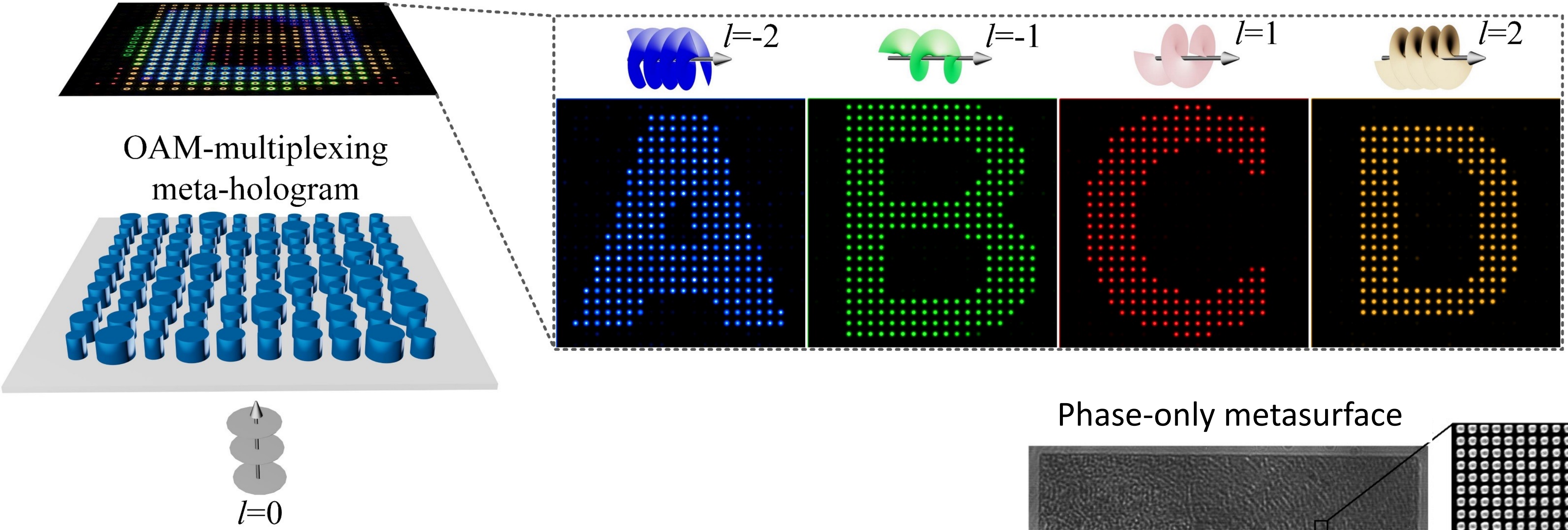

Phase-only metasurface

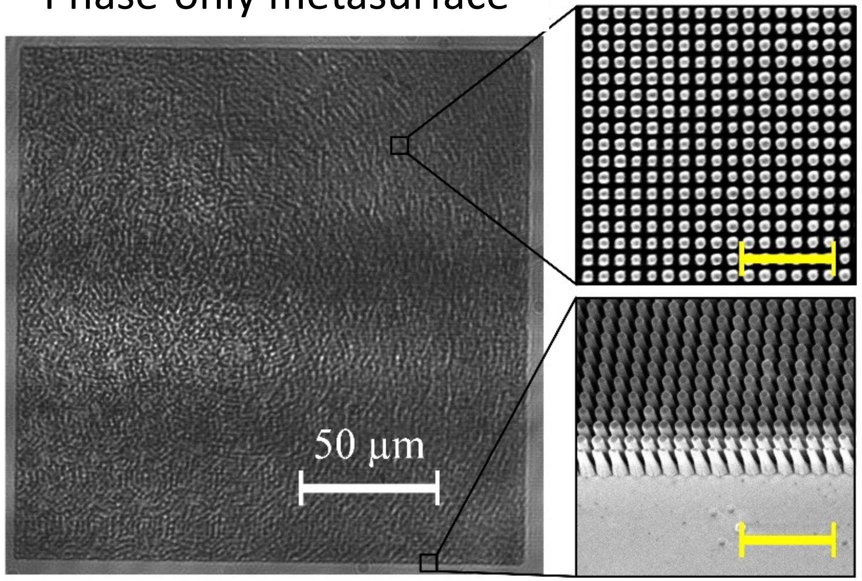

H. Ren, G. Briere, X. Fang, P. Ni, R. Sawant, S. Héron, S. Chenot, S. Vézian, B. Damilano, V. Brändli, S. A. Maier, P. Genevet, *Nat. Commun.* **10**, 2986 (2019).

Limitations of the OAM holography through phase-only holograms

Limitations of using a *phase-only* hologram for holographic multiplexing:

1) A breakdown of linear superposition principle for optical multiplexing (strong crosstalk).

2) Time-consuming phase retrieve methods.

Mathematical form of OAM multiplexing holography:

$$E^{mul} = \sum_{j=1}^{M} A_j e^{i\emptyset_j} e^{il_j\varphi} \qquad \mathcal{F}(E^{mul}) = \sum_{j=1}^{M} \mathcal{F}(A_j) \otimes \mathcal{F}(e^{i\emptyset_j}) \otimes \mathcal{F}(e^{il_j\varphi})$$

wherein A_j and $\emptyset_j$ stand for the amplitude and phase information of each image channel, respectively; $l_j \in \mathbb{Z}$ and φ represent the helical mode index and azimuthal angle, respectively, and M denotes the total number of multiplexing channels. $\mathcal{F}$ denotes the Fourier transform (FT) operator, expressing multiplexing results as the superposition of a convolution of the amplitude (A_j), phase ($\emptyset_j$), and encoded OAM (l_j) information of each image channel.

Phase-only approach:

$$P^{mul} = \arg\left[\sum_{j=1}^{M} e^{i\emptyset'_j} e^{il_j\varphi}\right] \qquad \mathcal{F}(P^{mul}) = \mathcal{F}(\arg\left[\sum_{j=1}^{M} e^{i\emptyset'_j} e^{il_j\varphi}\right])$$

Comparison of multiplexing results

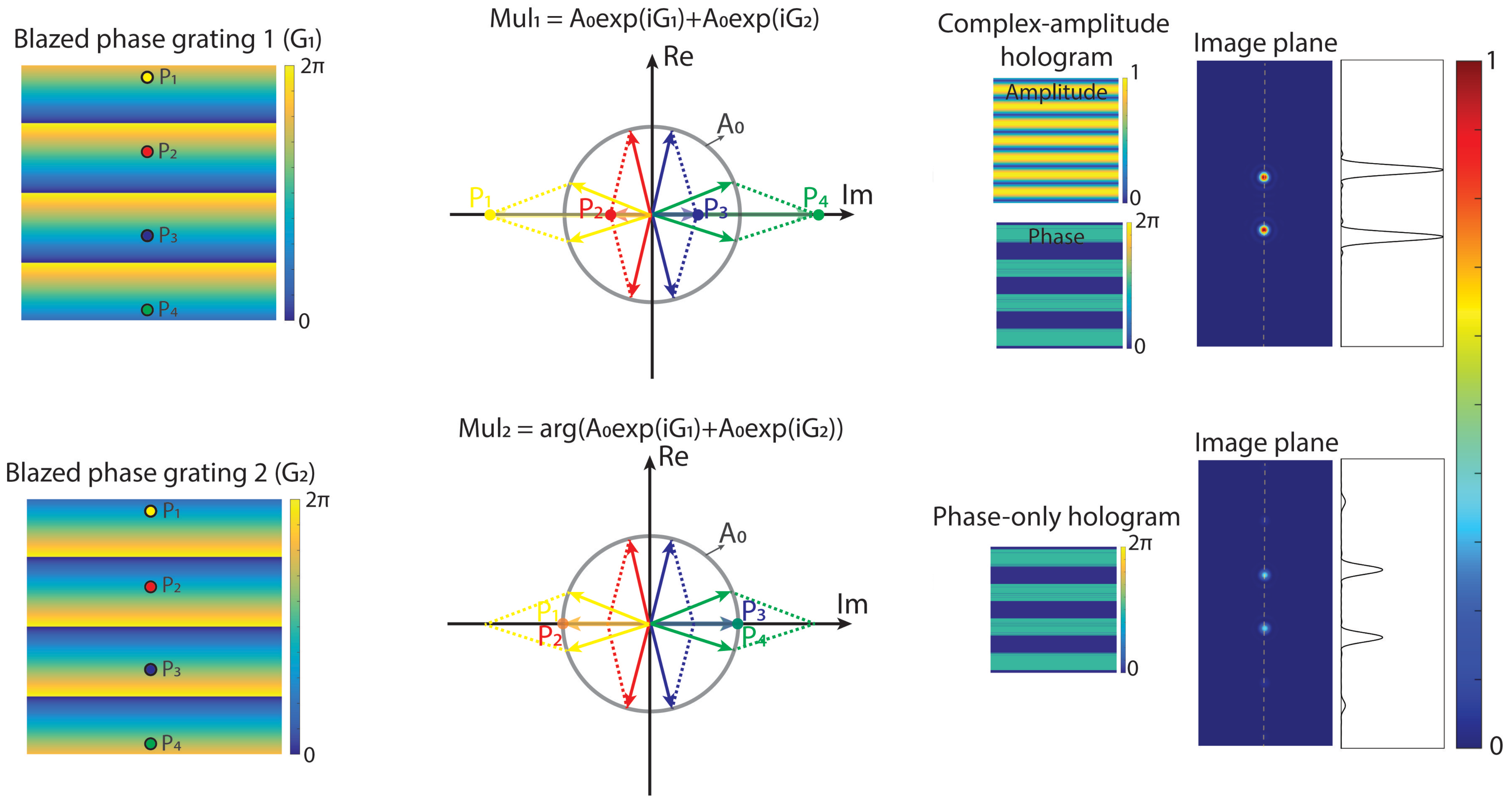

OAM holography via complex-amplitude metasurface holograms

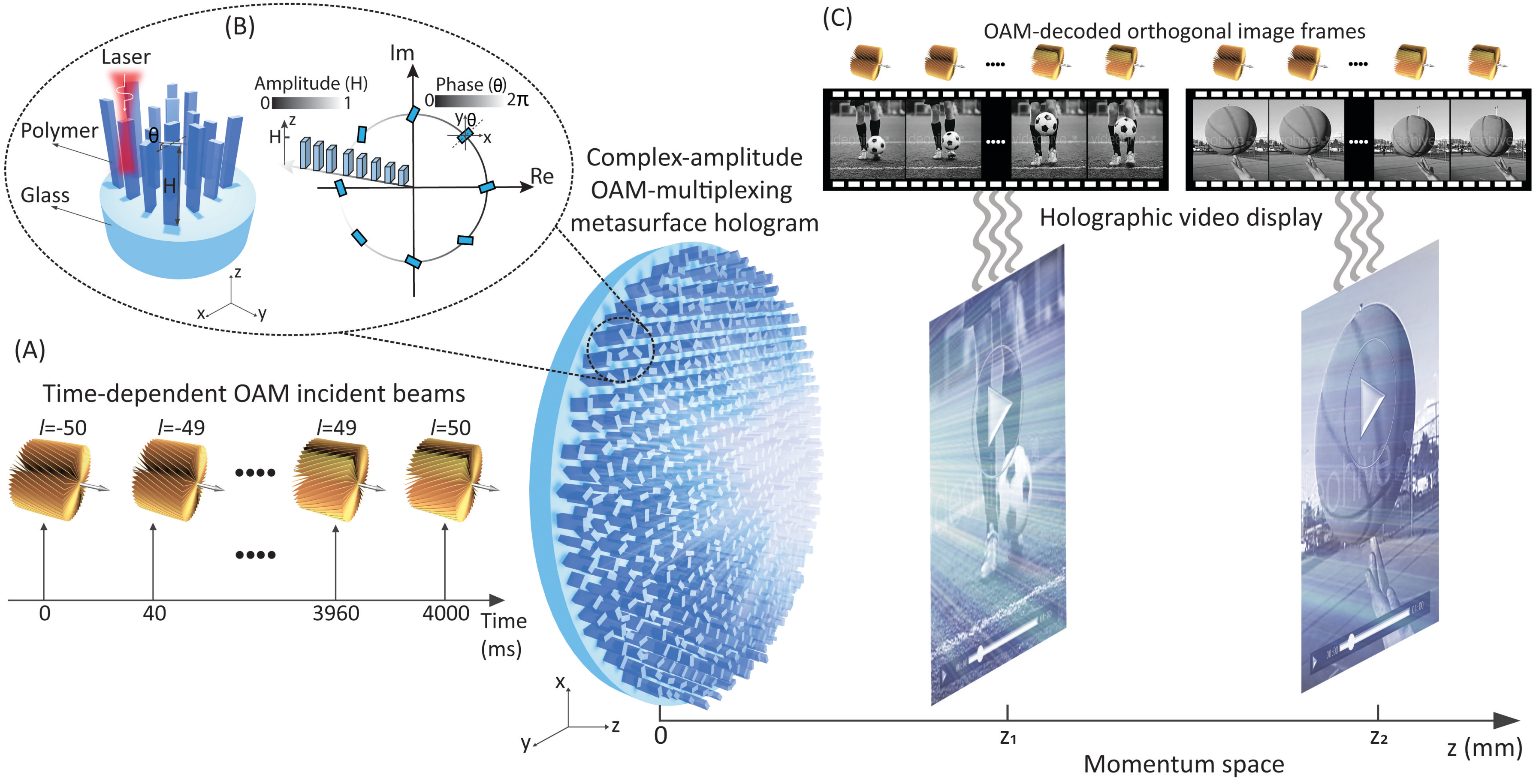

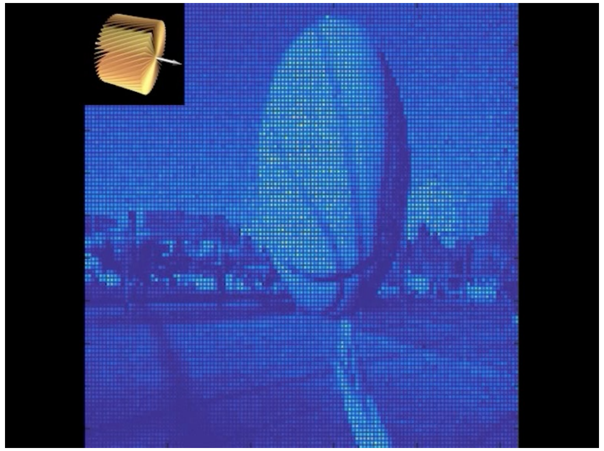

H. Ren, X. Fang, J. Jang, J. Burger, J. Rho, and S. A. Maier, Complex-amplitude metasurface-based orbital angular momentum holography in momentum space, ***Nat. Nanotechnol.*** **15**, 948-955 (2020).

Design of a complex-amplitude hologram

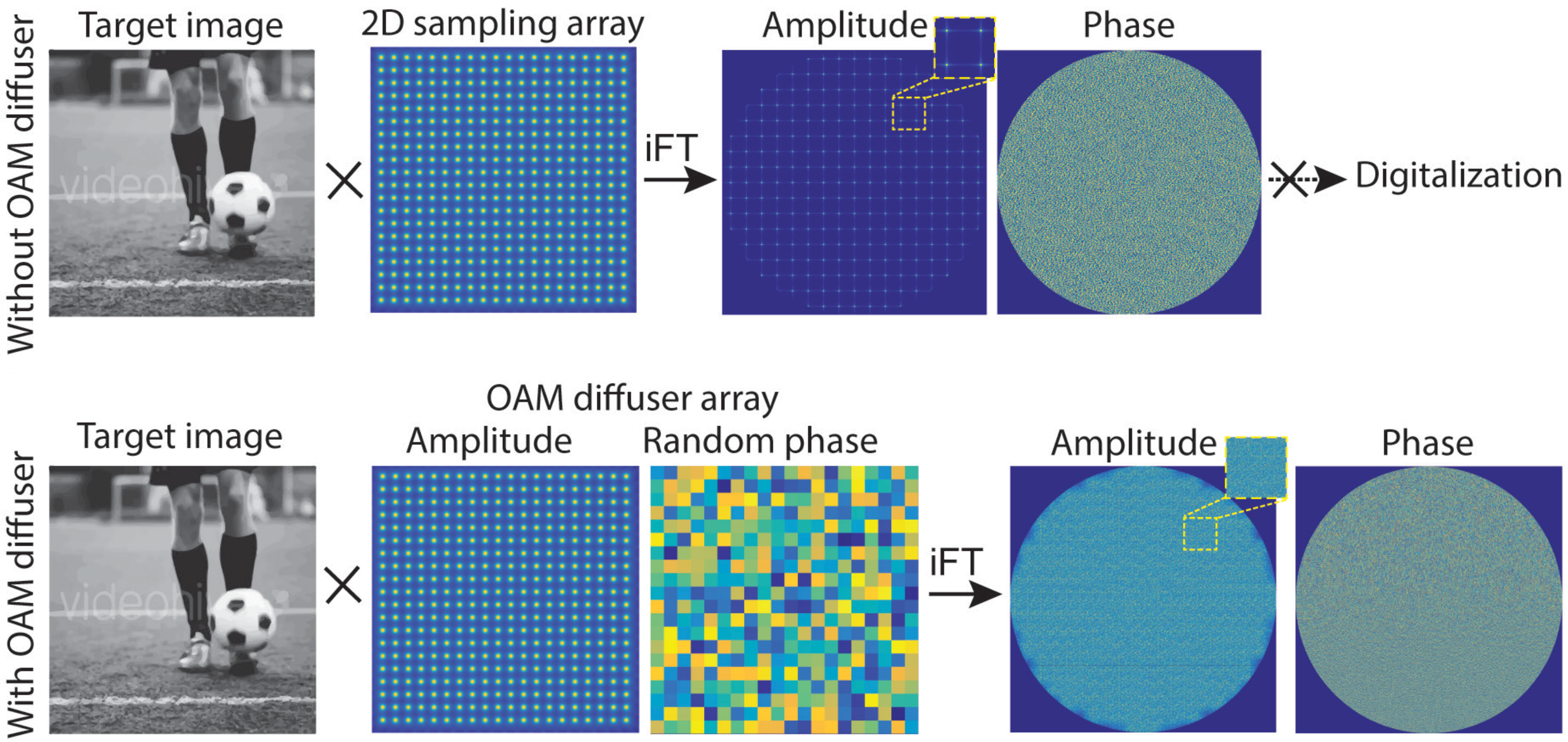

H. Ren, X. Fang, J. Jang, J. Burger, J. Rho, and S. A. Maier, Complex-amplitude metasurface-based orbital angular momentum holography in momentum space, *Nat. Nanotechnol.* **15**, 948-955 (2020).

Design of a complex-amplitude hologram

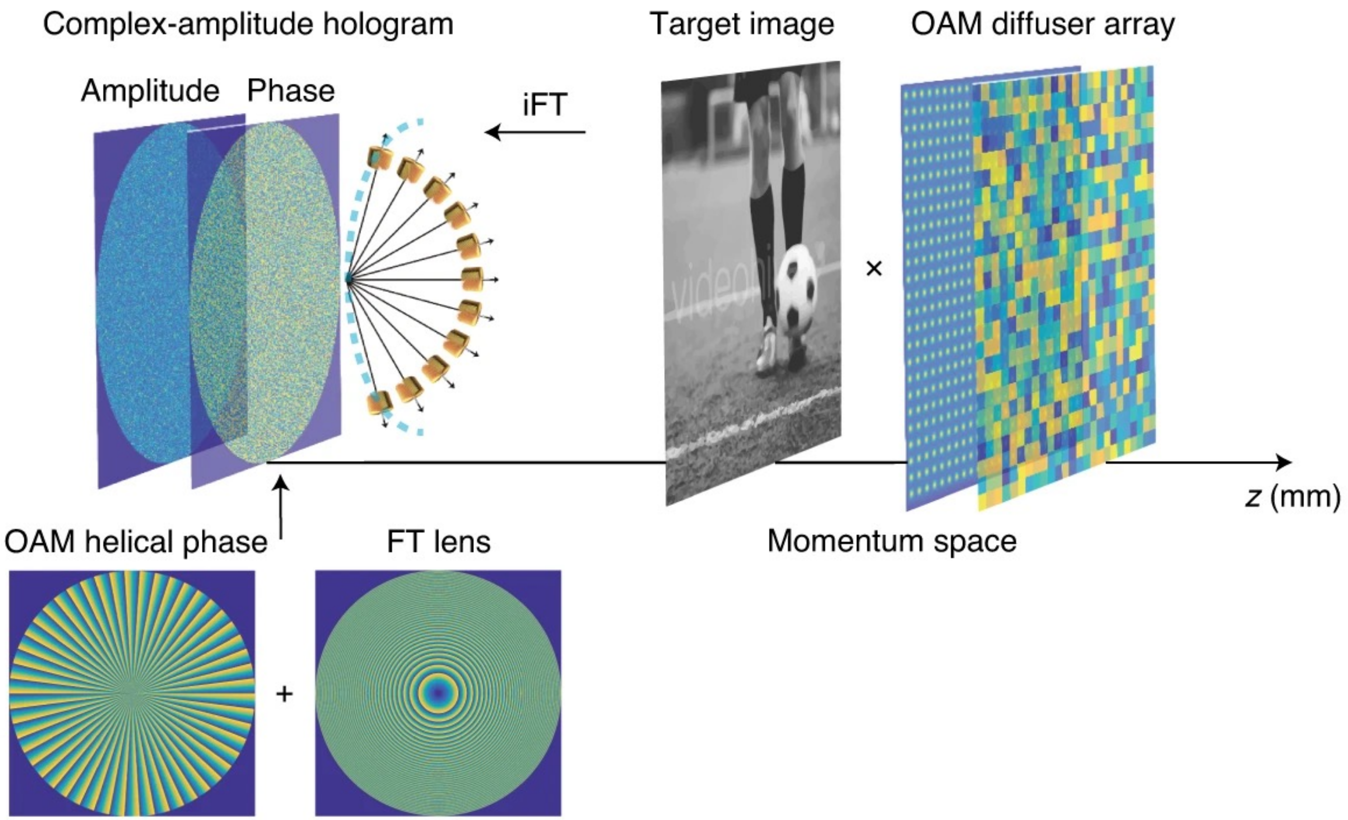

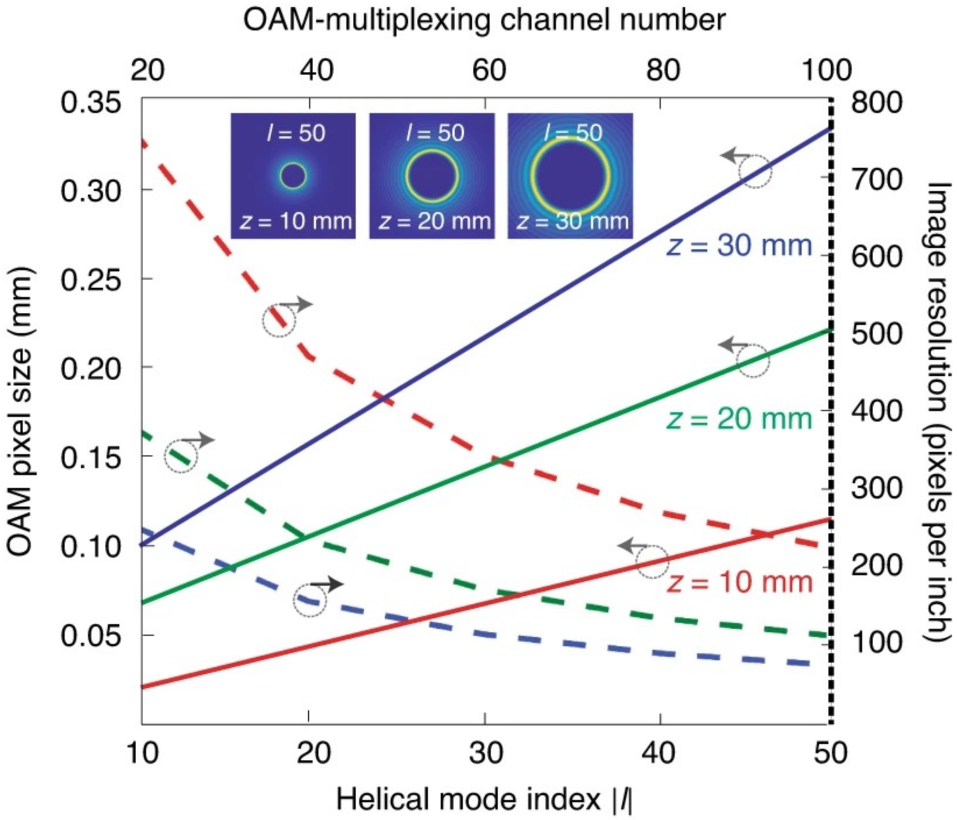

H. Ren, X. Fang, J. Jang, J. Burger, J. Rho, and S. A. Maier, Complex-amplitude metasurface-based orbital angular momentum holography in momentum space, *Nat. Nanotechnol.* **15**, 948-955 (2020).

3D meta-optics for complex-amplitude modulation

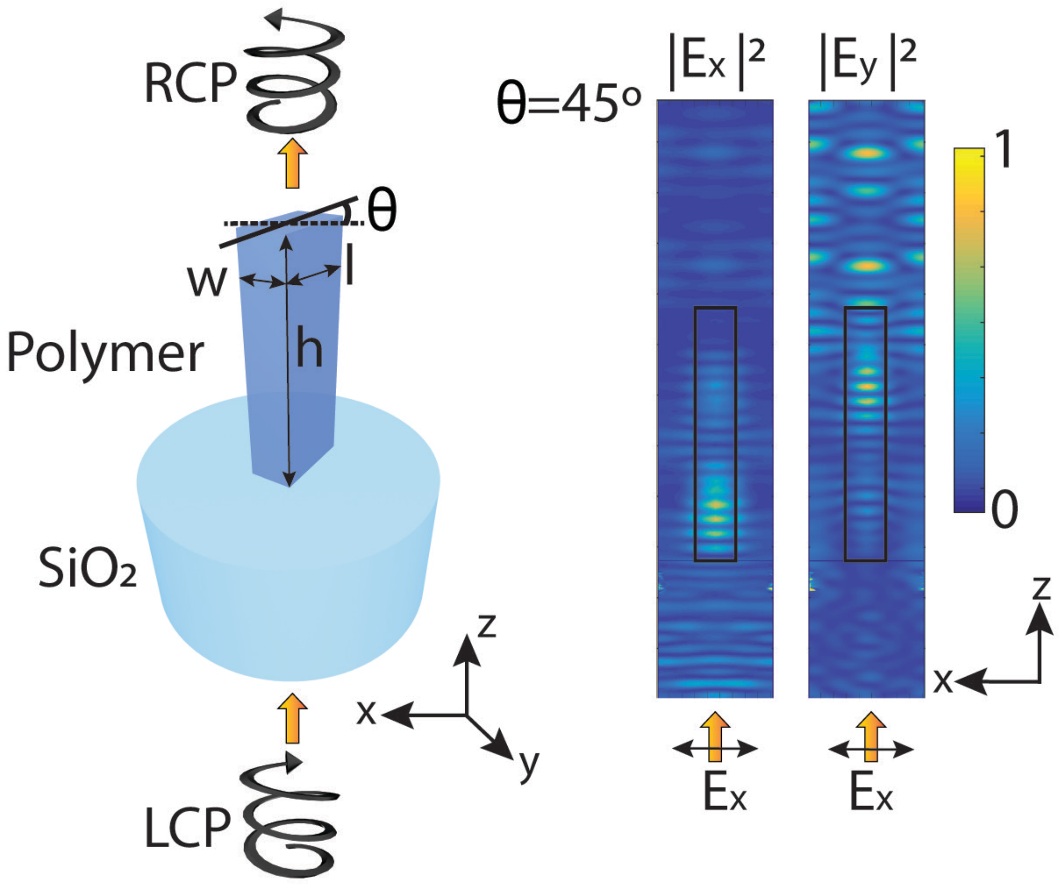

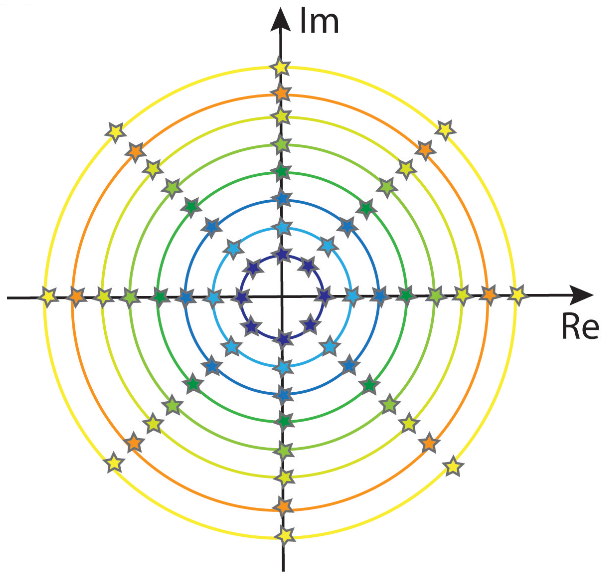

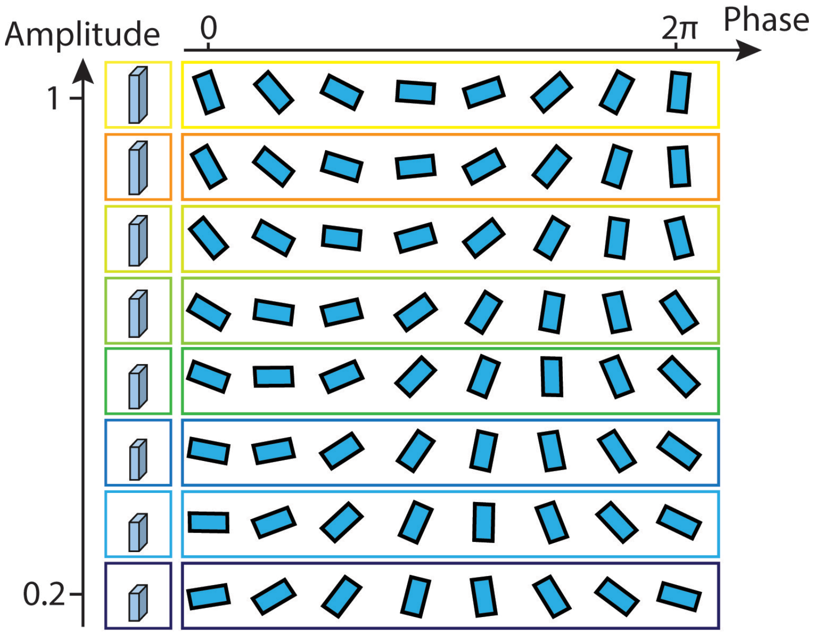

H. Ren, X. Fang, J. Jang, J. Burger, J. Rho, and S. A. Maier, Complex-amplitude metasurface-based orbital angular momentum holography in momentum space, *Nat. Nanotechnol*. **15**, 948-955 (2020).

High-aspect-ratio 3D nanopillar waveguides

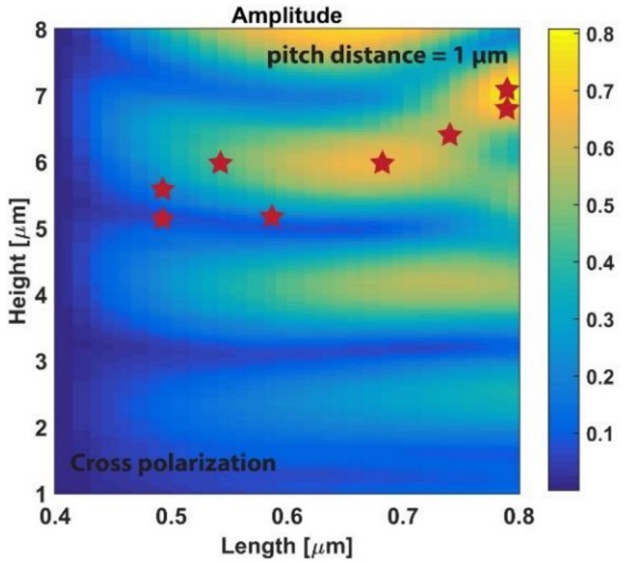

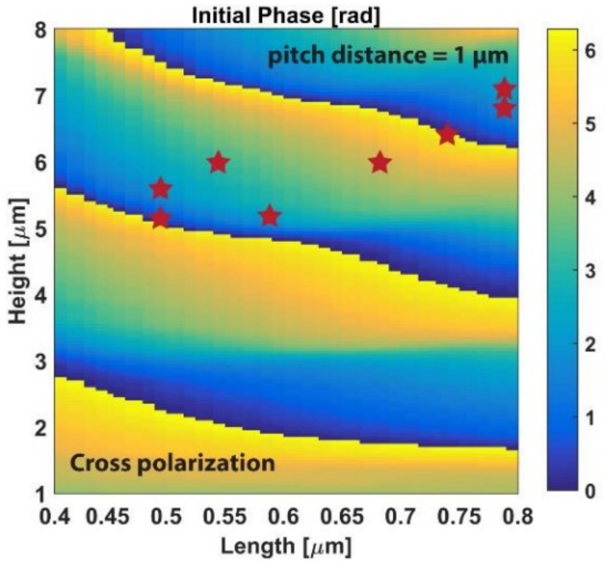

H. Ren, X. Fang, J. Jang, J. Burger, J. Rho, and S. A. Maier, Complex-amplitude metasurface-based orbital angular momentum holography in momentum space, *Nat. Nanotechnol*. **15**, 948-955 (2020).

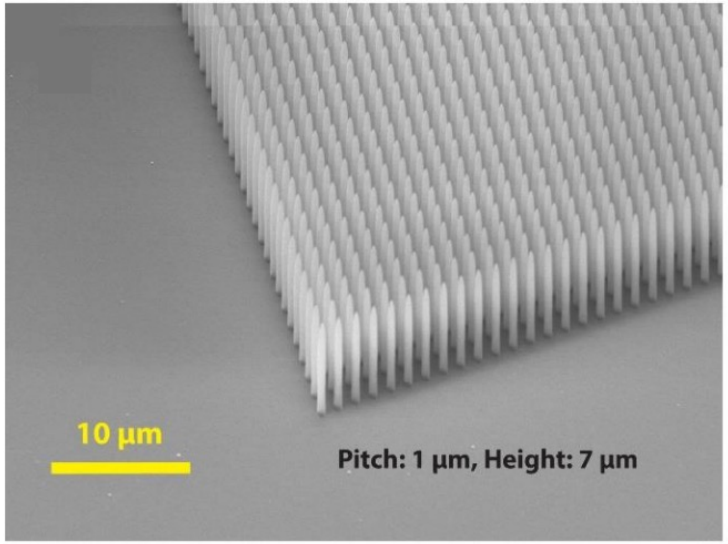

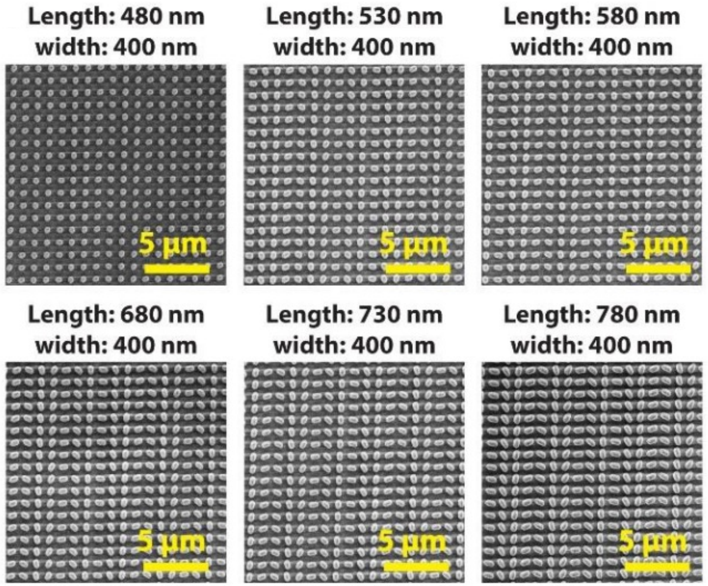

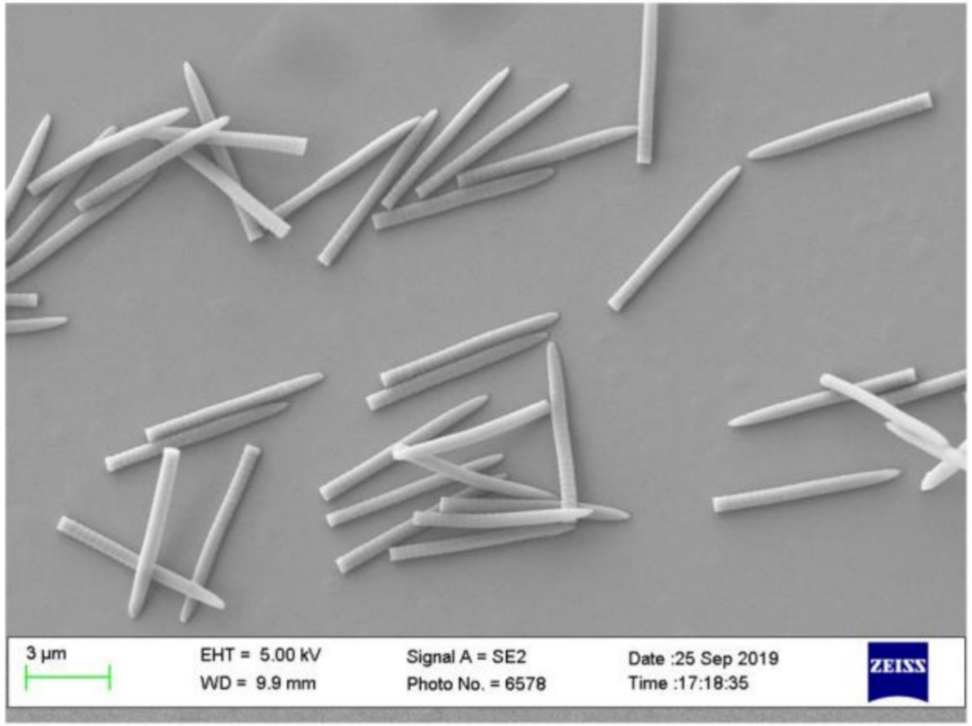

OAM holography based on a complex-amplitude metasurface

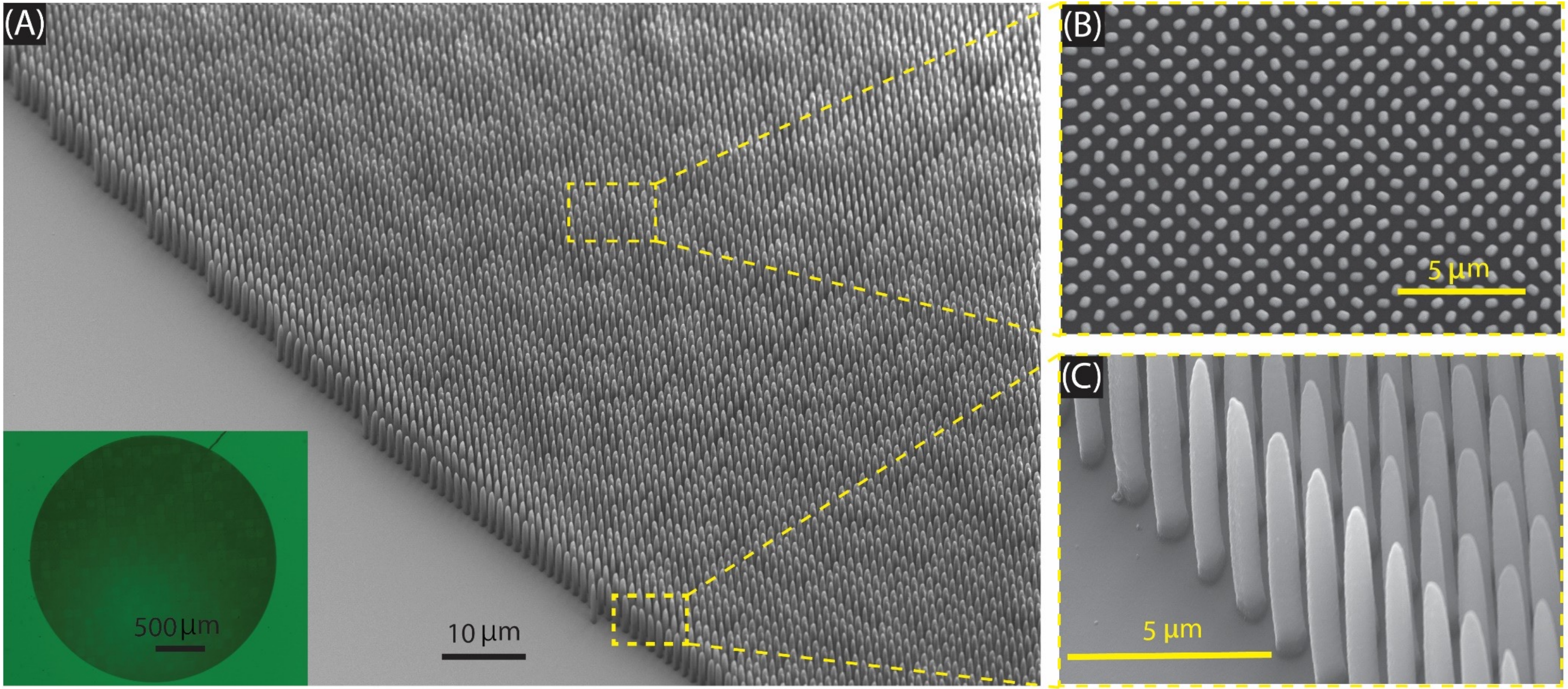

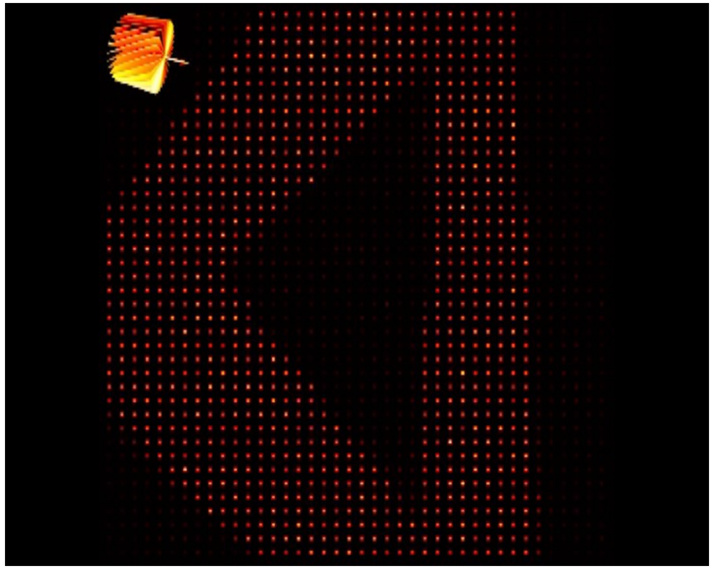

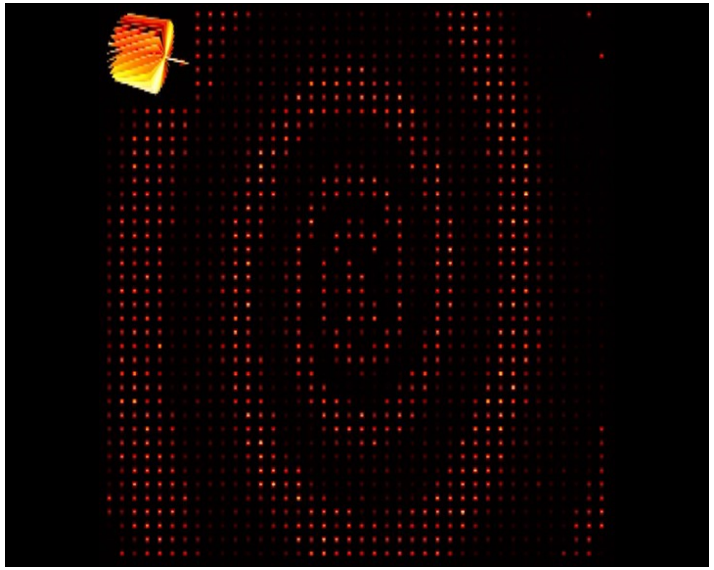

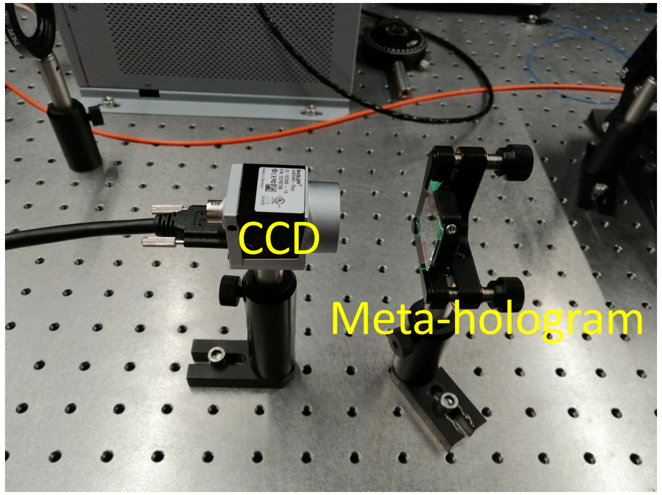

H. Ren, X. Fang, J. Jang, J. Burger, J. Rho, and S. A. Maier, Complex-amplitude metasurface-based orbital angular momentum holography in momentum space, *Nat. Nanotechnol.* **15**, 948-955 (2020).

•Outline

- Complex-amplitude metasurface for twisted light holography

- Plasmonic nanofin metasurface for tailored molecular sensing

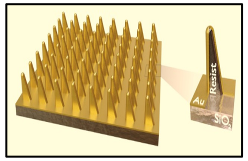

- Achromatic metafibre for broadband focusing and imaging

High Q-factor bound states in the continuum (BIC)

Accidental BIC resonances

Off-Γ Friedrich-Wintgen accidental BICs
Radiation loss vanishes due to total destructive interference of two modes

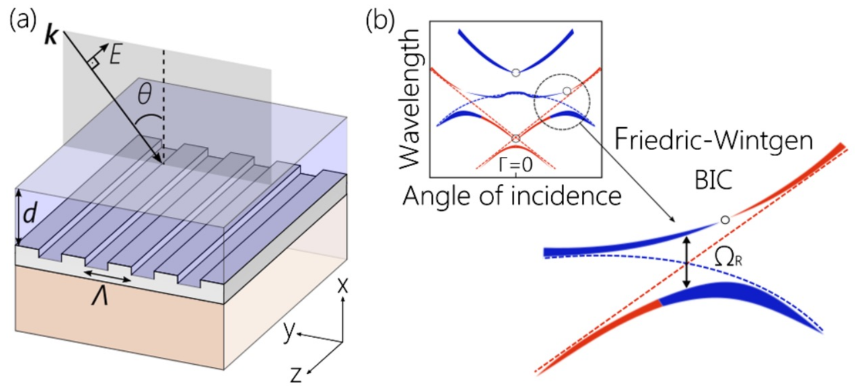

S. I. Azzam, PRL **121**, 253901 (2018)

Symmetry-protected BIC resonances

Radiation vanishes as a result of symmetry mismatch

$$Q = \frac{w_0}{2\gamma_{\text{rad}}}$$

For $\gamma_{rad} \to 0$
$Q \to \infty$

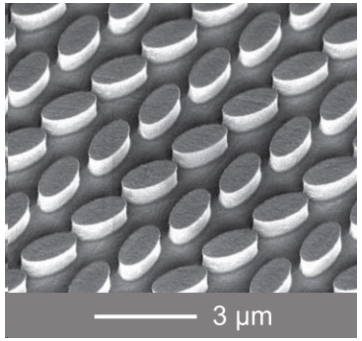

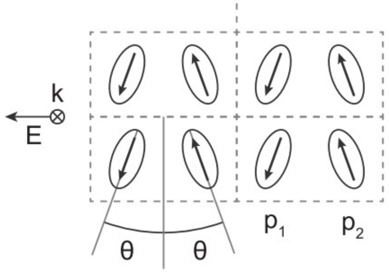

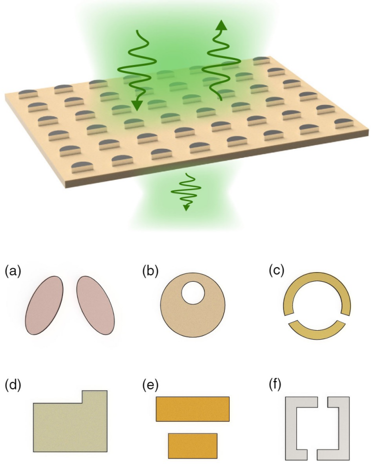

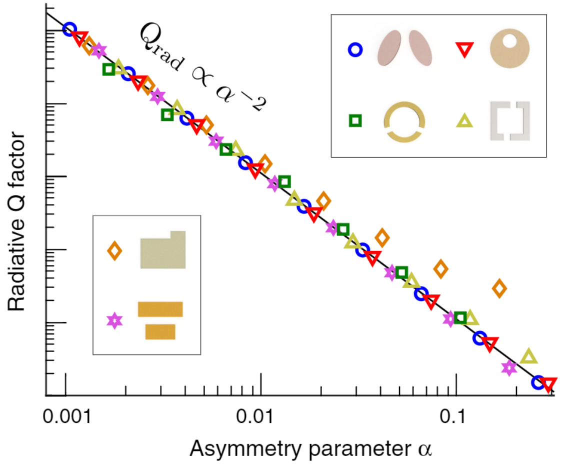

K. Koshelev et al, Phys. Rev. Lett. **121**, 193903 (2018)

A. Tittl, Science **360**, 1105-1109 (2018)

Essential pathways for molecular sensing

Surface field-enhanced plasmonic metasurfaces

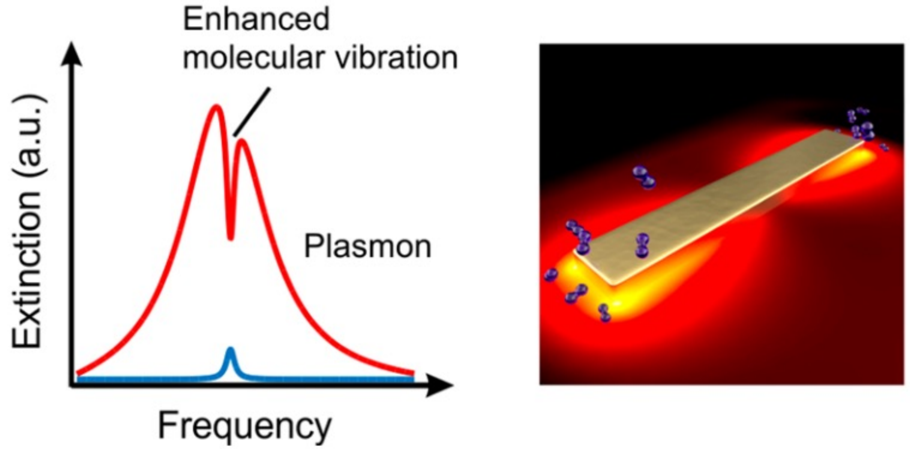

F. Neubrech, et. al. *Chem. Rev.* 117, 7 (2017).

High Q-factor dielectric BIC metasurfaces

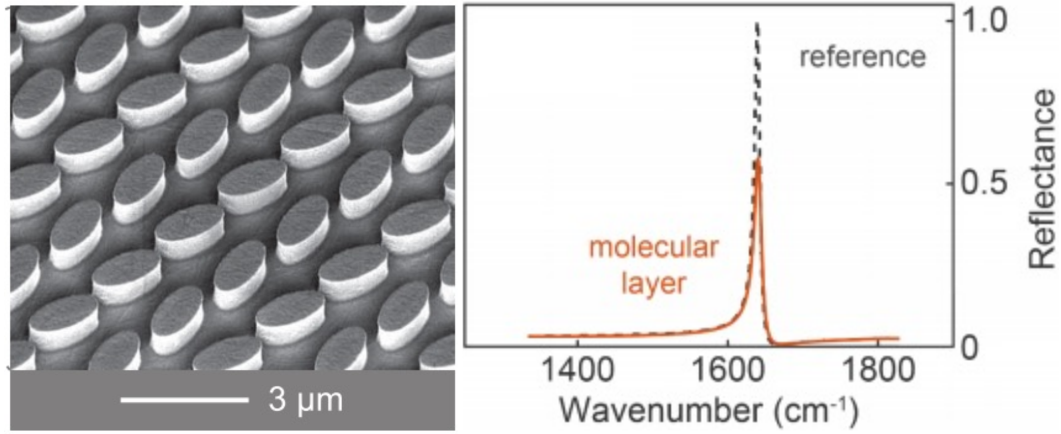

A. Tittl, et. al. *Science* 360, 6393 (2018).

Strong light-matter interaction

Plasmonic nanofin metasurface

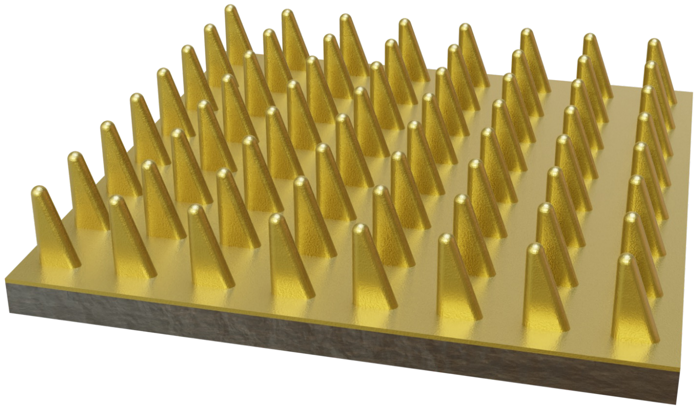

High Q-factors

Plasmonic resonances

Also see: *Phys. Rev. Lett.* **121**,253901 (2018).

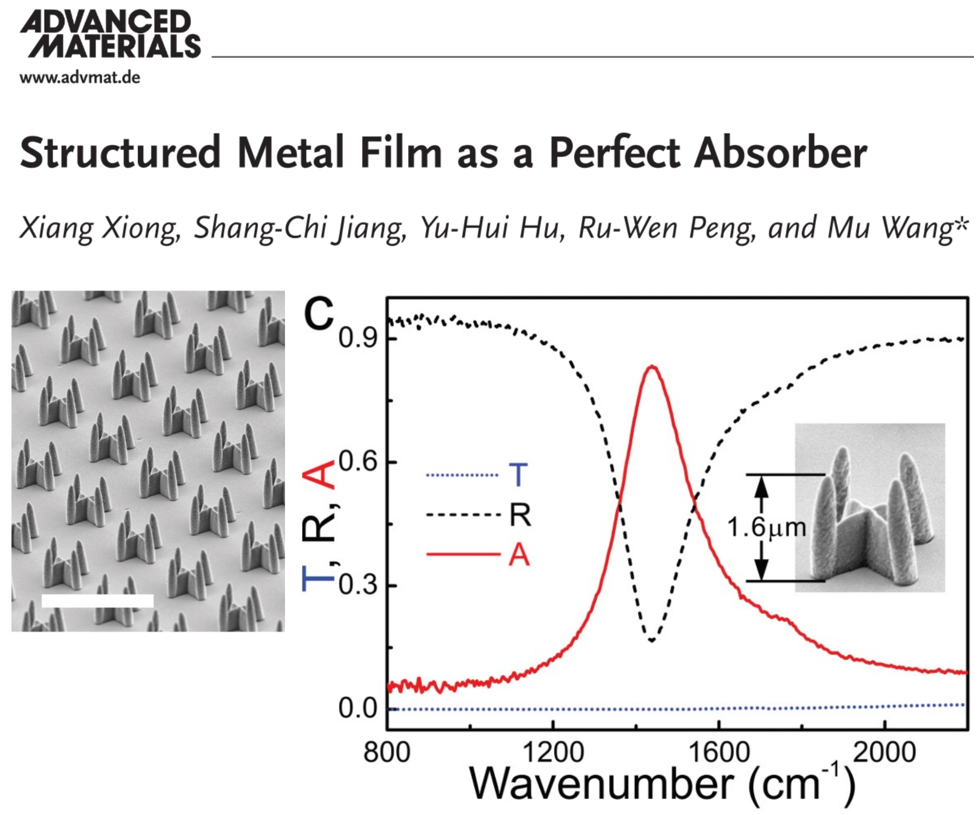

Gold coated polymer structure
Perfect Mid-IR absorption
Resonance frequency is tunable by the height

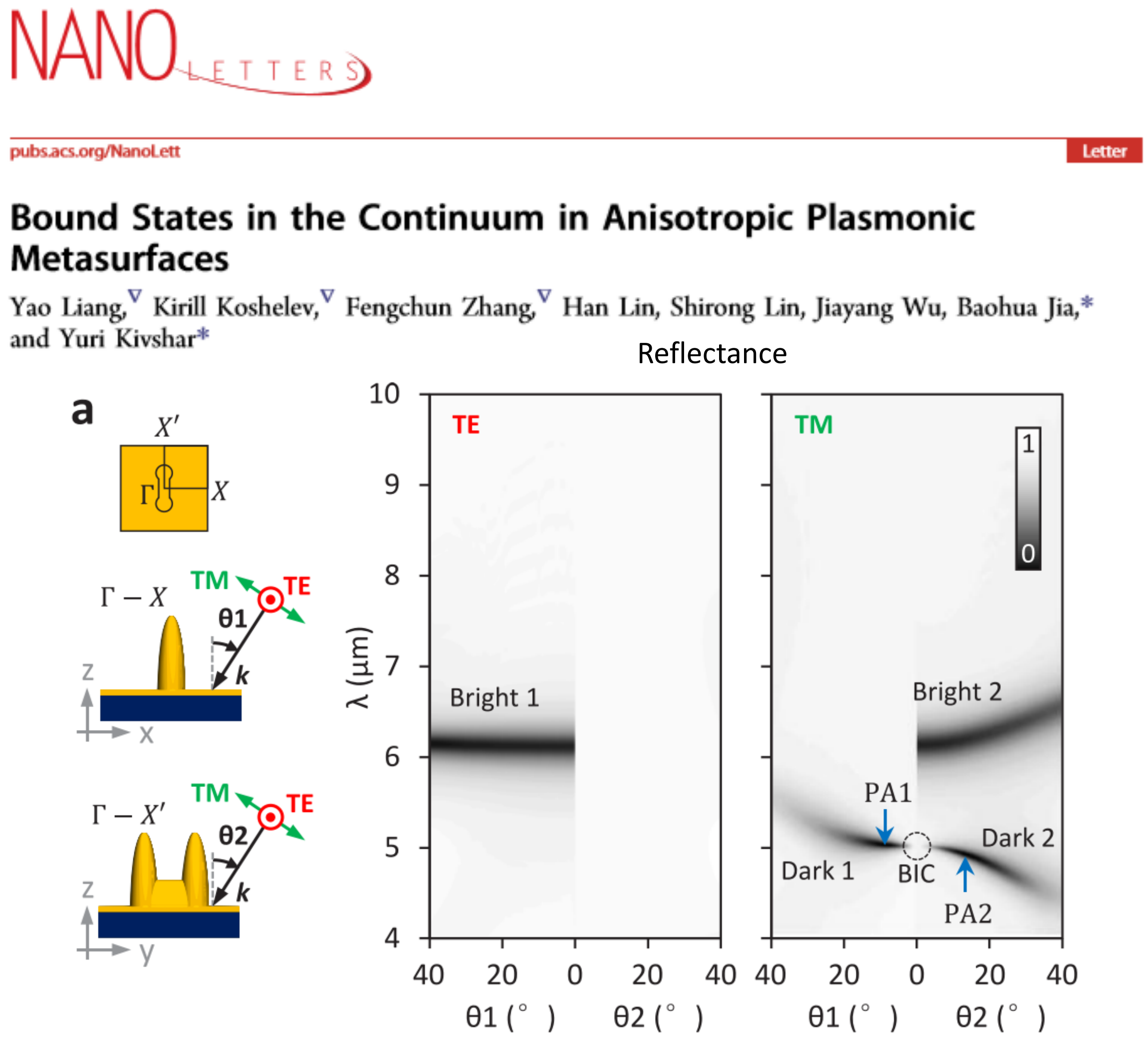

Out-of-plane symmetry-protected BIC

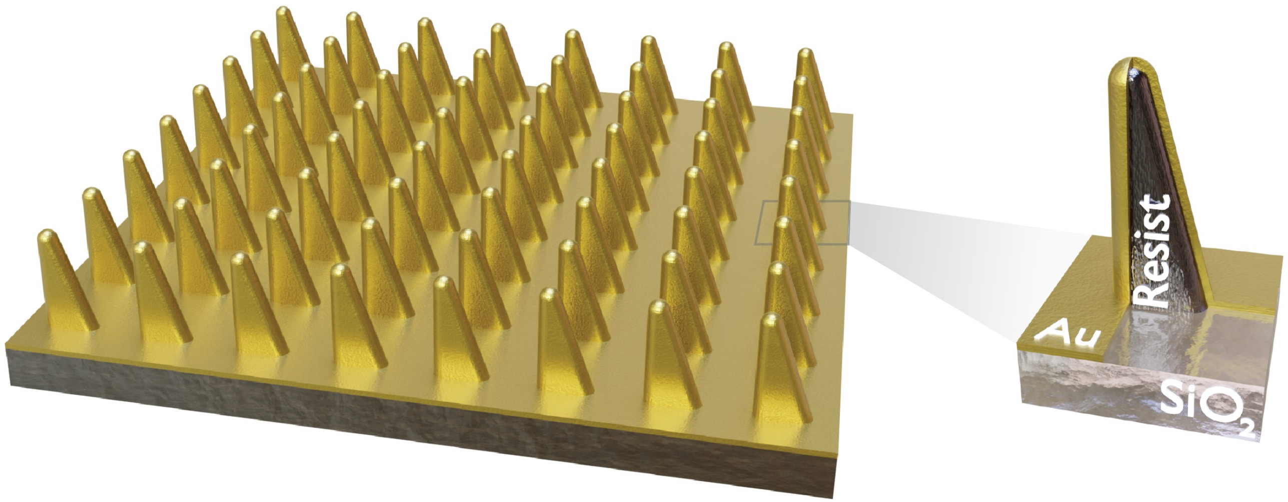

Arrays of gold coated standing triangular nanofins

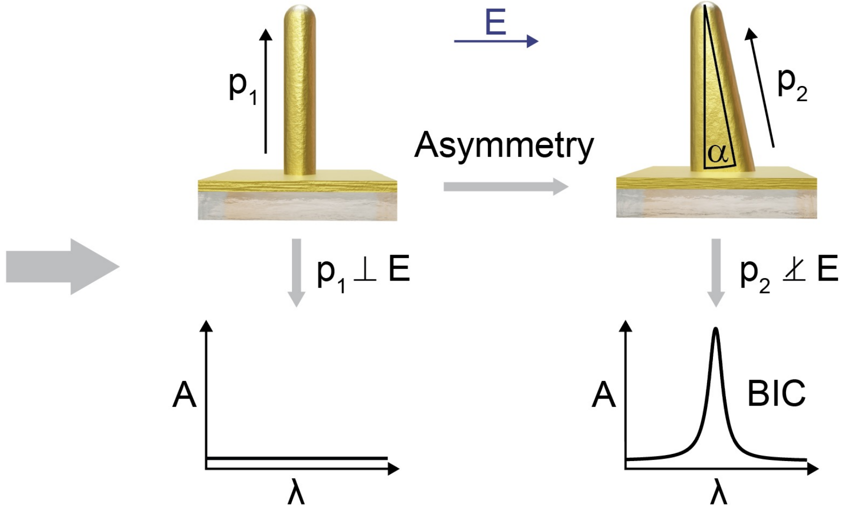

Net dipole moment between asymmetric structure and the electric field

A. Aigner, A. Tittl, J. Wang, T. Weber, Y. Kivshar, S. A. Maier, and H. Ren, Plasmonic bound states in the continuum to tailor light-matter coupling, *Sci. Adv*. **8**, eadd4816 (2022).

Out-of-plane symmetry-protected BIC

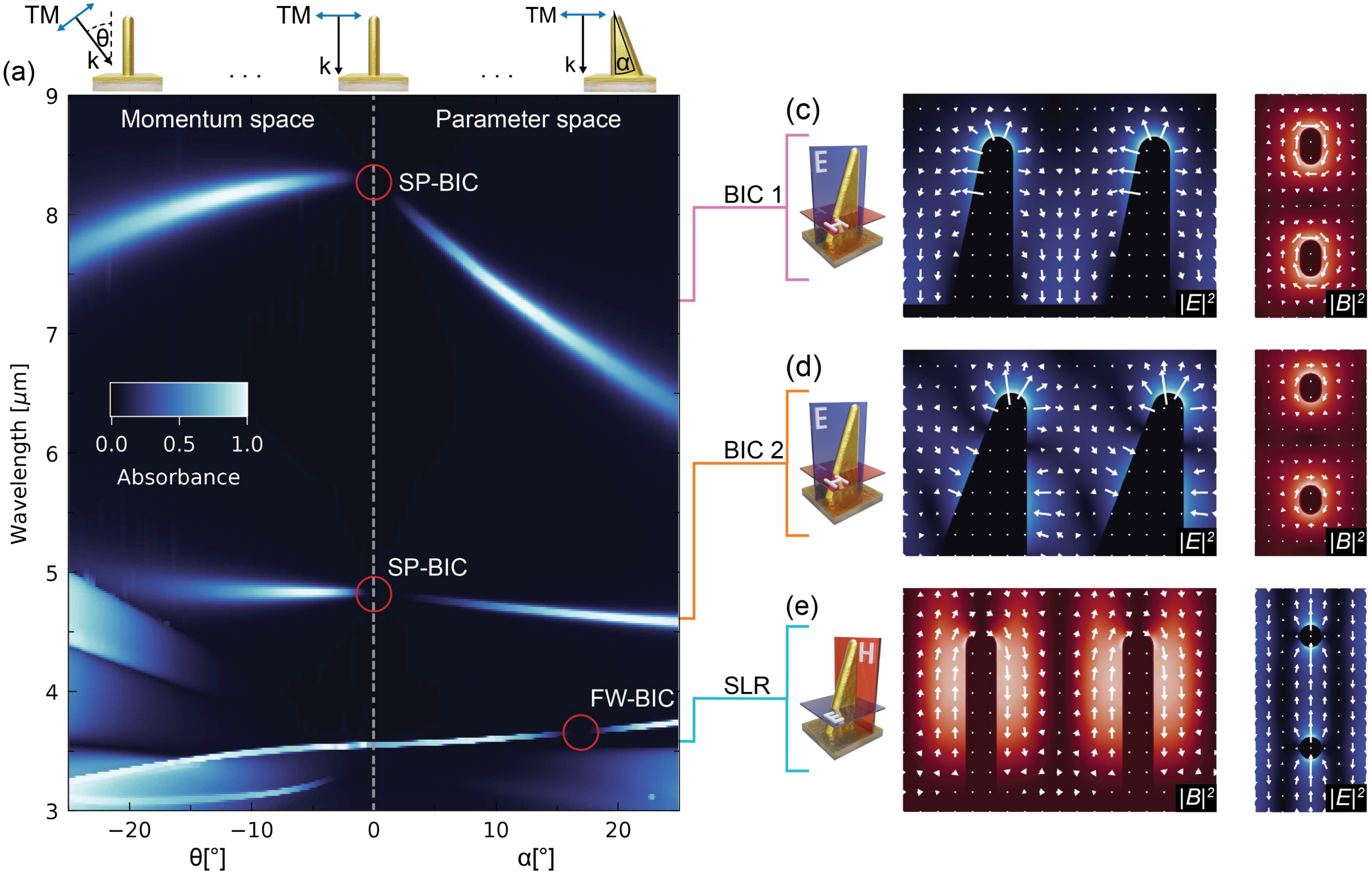

Tailoring light-matter coupling in a plasmonic nanofin metasurface

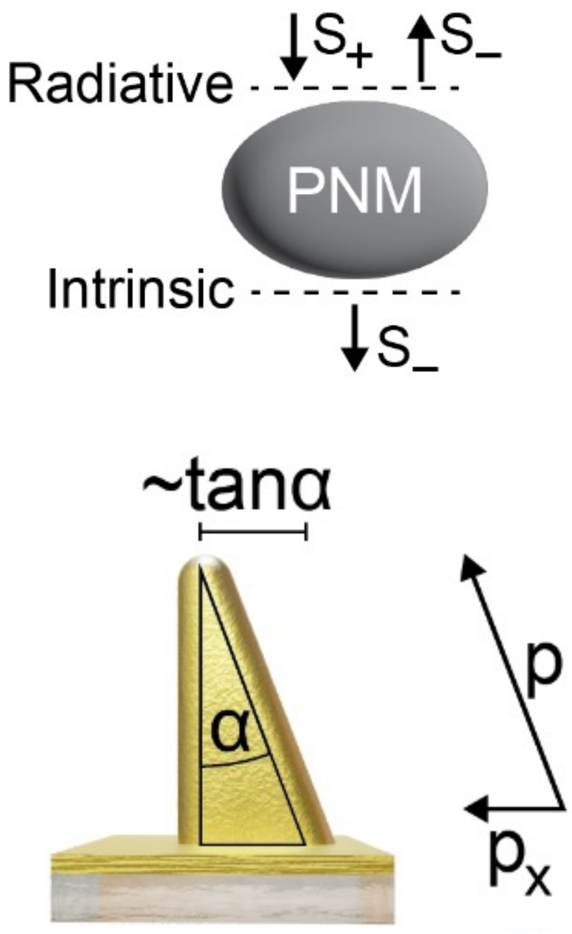

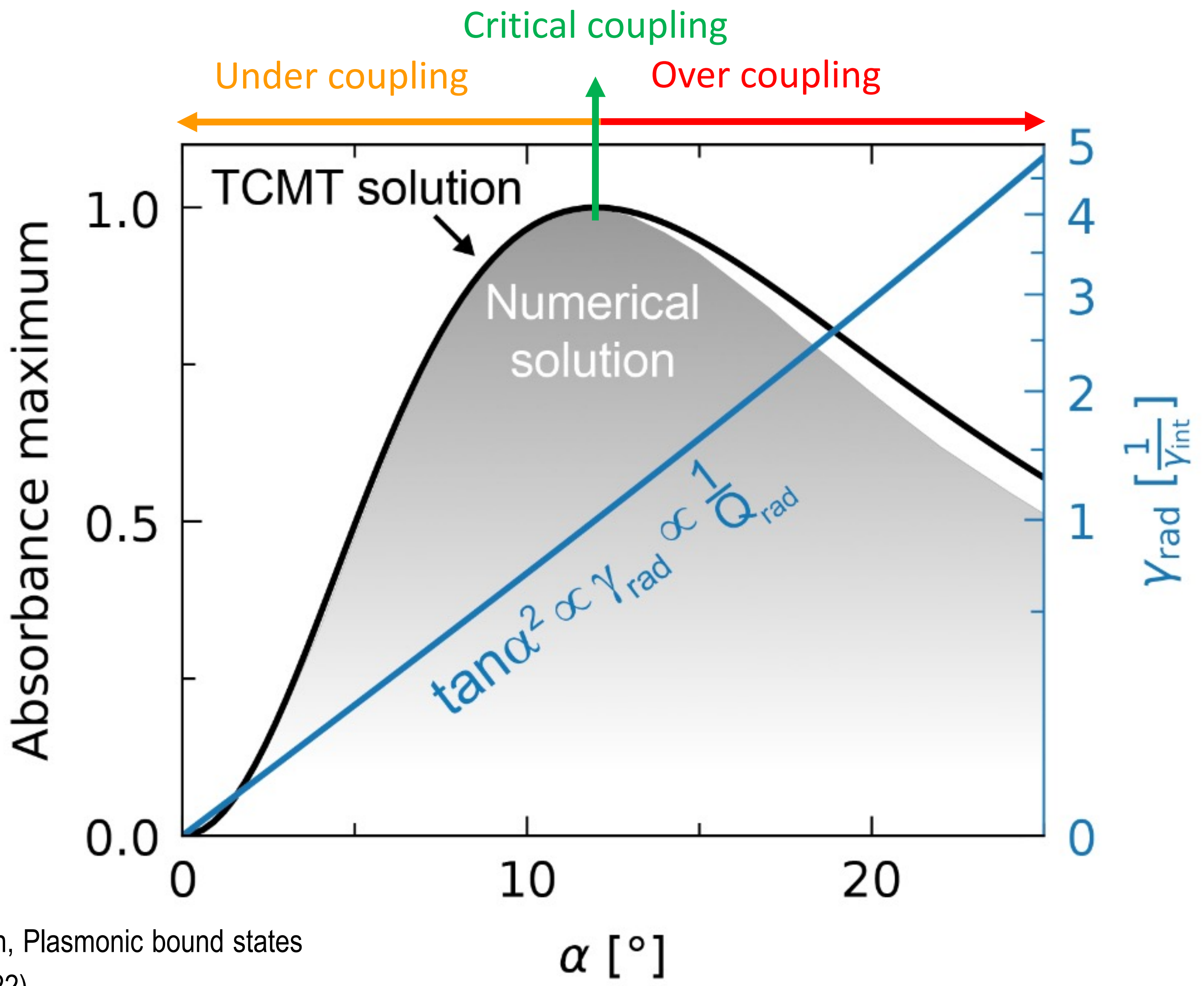

A. Aigner, A. Tittl, J. Wang, T. Weber, Y. Kivshar, S. A. Maier, and H. Ren, Plasmonic bound states in the continuum to tailor light-matter coupling, *Sci. Adv*. **8**, eadd4816 (2022).

Fabrication and experimental verification of higher-order BICs

Fabrication

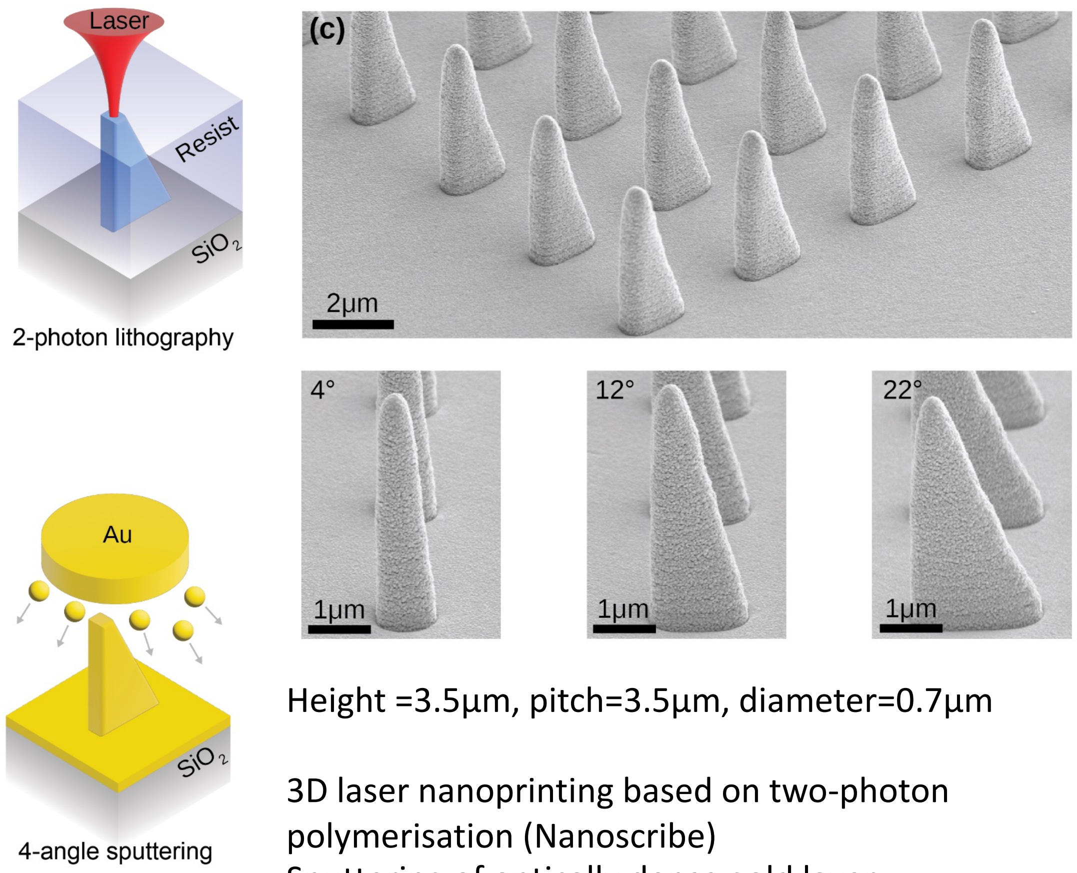

Height =3.5µm, pitch=3.5µm, diameter=0.7µm

3D laser nanoprinting based on two-photon polymerisation (Nanoscribe)
Sputtering of optically dense gold layer

Simulation vs. experiment

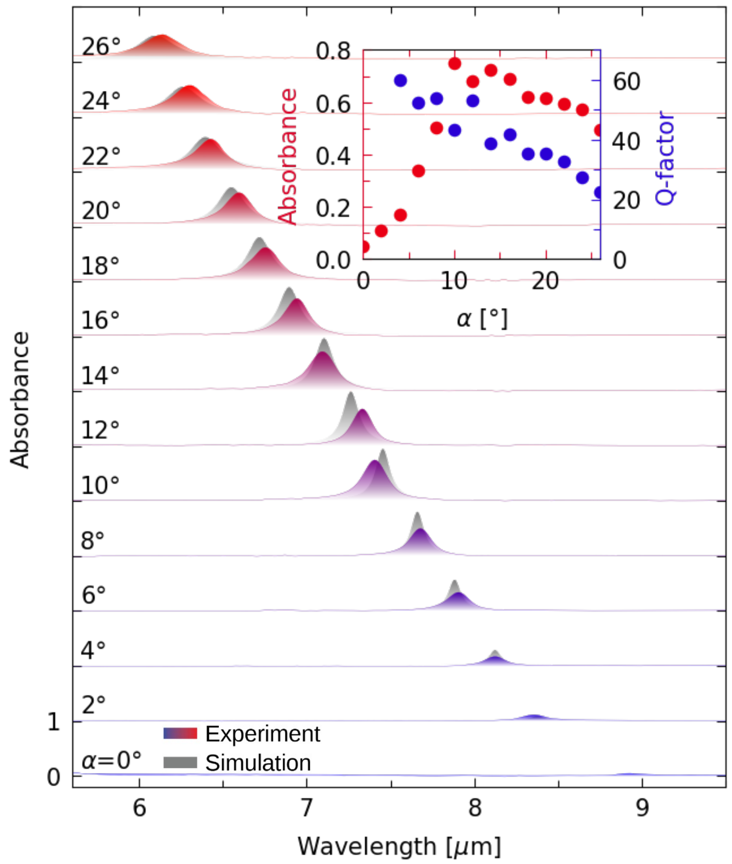

Mid-IR spectral imaging microscope (Spero)
Good agreement of simulation with experiment

A. Aigner, A. Tittl, J. Wang, T. Weber, Y. Kivshar, S. A. Maier, and H. Ren, Plasmonic bound states in the continuum to tailor light-matter coupling, *Sci. Adv*. **8**, eadd4816 (2022).

Four-angle gold sputtering

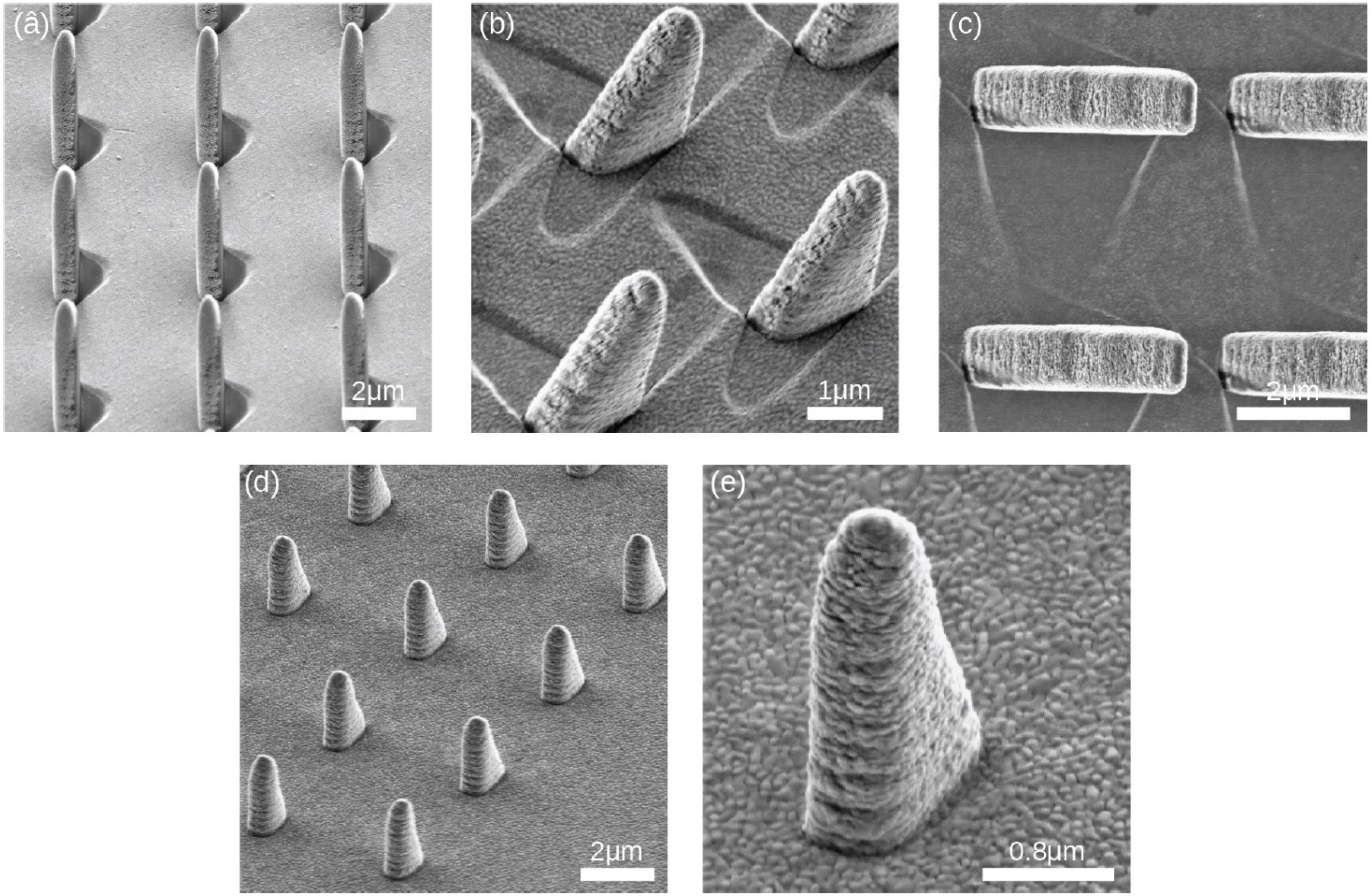

Figure 3.6: Thermal Evaporation vs. Sputtering. (a) shows Nano-Fins from the side with 100 nm thermal evaporated gold at a slight angle (no wedge used). The darker areas indicate were no gold is deposited. The Nano-Fins in (b,c) are coated by four-step thermal evaporation (160 nm in total), and in (d,e) they have a four-step sputtering 160 nm gold coating.

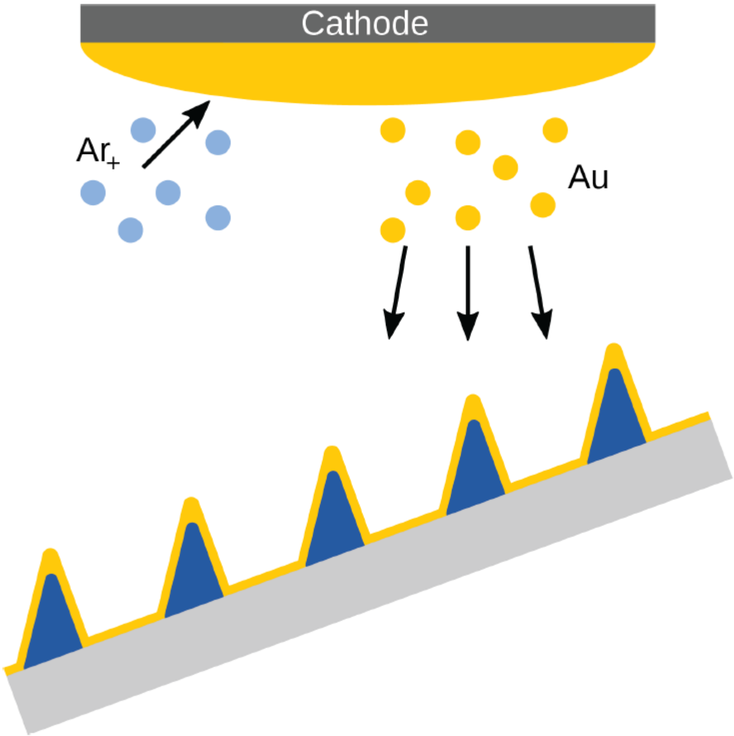

Light-matter coupling-tailored molecular sensing

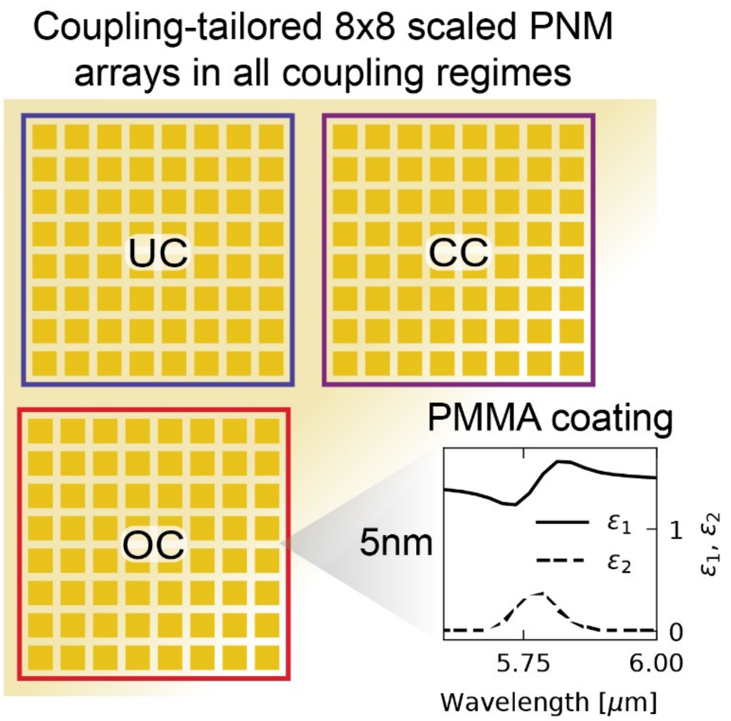

Simulation: 5nm even coating.
Experiment: Spin-coating of A1 PMMA & 5000rpm

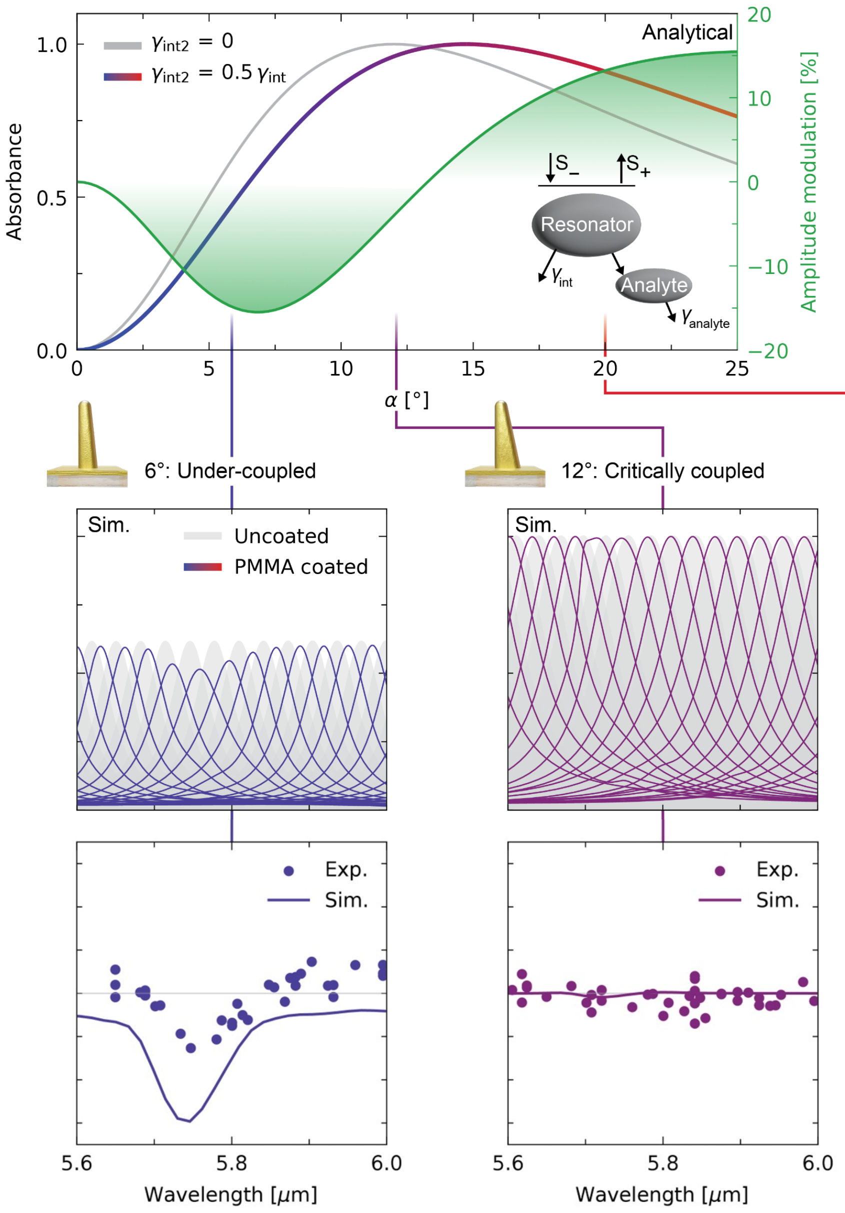

- Additional intrinsic loss shifts critical coupling condition
- Amplitude modulation depends on coupling regimes
- Field enhancement is of secondary importance for molecular sensing

A. Aigner, A. Tittl, J. Wang, T. Weber, Y. Kivshar, S. A. Maier, and H. Ren, Plasmonic bound states in the continuum to tailor light-matter coupling, *Sci. Adv*. **8**, eadd4816 (2022).

•Outline

- Complex-amplitude metasurface for twisted light holography

- Plasmonic nanofin metasurface for tailored molecular sensing

- Achromatic metafibre for broadband focusing and imaging

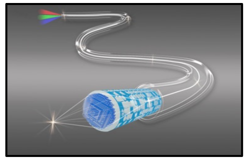

Metafibre optics for fibre functionalisation

An achromatic metafibre for focusing and imaging across the entire telecommunication range

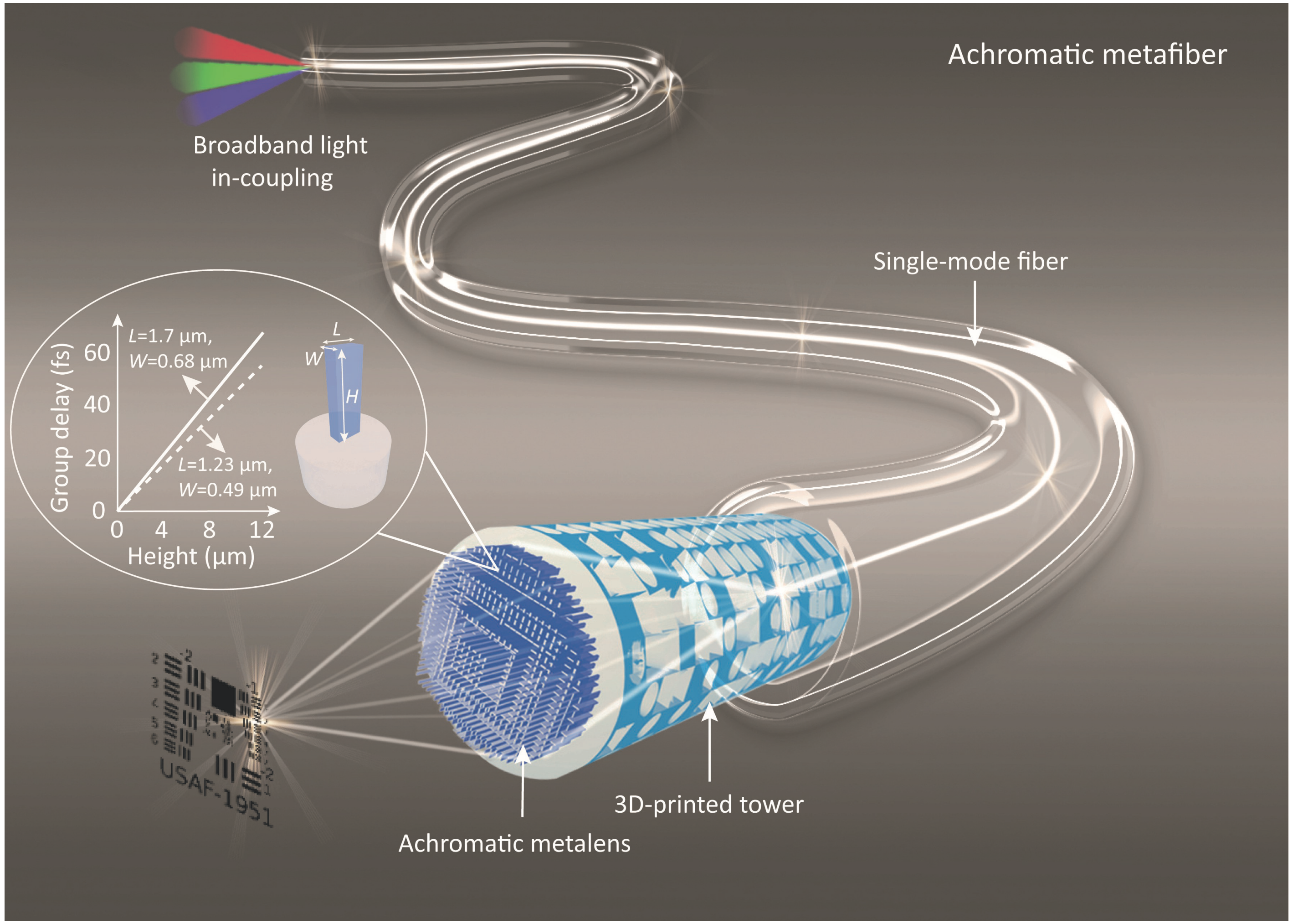

For more technical details, please come to my talk at **3pm today at Hall A**

H. Ren, J. Jang, C. Li, A. Aigner, M. Plidschun, J. Kim, J. Rho, M. A. Schmidt, and S. A. Maier, An achromatic metafiber for focusing and imaging across the entire telecommunication range, ***Nat. Commun.***, 13, 4183 (2022).

MONASH University

Acknowledgement

LMU Munich, Germany
Andreas Aigner
Stefan A. Maier (now at **Monash**)

POSTECH, South Korea
Jaehyuck Jang
Junsuk Rho

CNRS, France
Patrice Genevet

USST, China
Xinyuan Fang
Min Gu